# Hybrid model of PMSG based WECS with PV array connected to the grid using back-to-back converter

*A thesis is submitted to fulfill the requirement of the degree*

**Master in Electrical Engineering**

Submitted by
**Pritam Kumar**
Examination Roll no. – M4ELE22009
Registration no. –153999 Of **2020-2021**

Under the guidance of
**Dr. Debashis Chatterjee**
**Prof. Nikhil Mondal**
And
**Prof. Mihir Hembram**

Department of Electrical Engineering
Jadavpur University
Kolkata – 700032
June, 2022

# Faculty of Engineering and Technology
# Jadavpur University, Kolkata - 700032

## Certificate

This is to certify that the thesis entitled "**Hybrid model of PMSG based WECS with PV Array connected to the grid using back-to-back converter**", submitted by **Mr. Pritam Kumar** (Examination Roll No. M4ELE22009 ), under our supervision and guidance during the session of 2020-22 in the department of Electrical Engineering, Jadavpur University. We are satisfied with his work, which is being presented for the partial fulfilment of the degree of **Master in Electrical Engineering** from Jadavpur University,Kolkata-700032.

……..
**Dr. Debashis Chatterjee**
Professor
Department of Electrical Engineering
Jadavpur University
Kolkata, 700032

……
**Prof. Nikhil Mondal**
Associate Professor
Department of Electrical Engineering
Jadavpur University
Kolkata, 700032

.....
**Prof. Mihir Hembram**
Assistant Professor
Department of Electrical Engineering
Jadavpur University
Kolkata, 700032

……
**Prof. Chandan Mazumdar**
Dean of Faculty Council of
Engineering and Technology
Jadavpur University
Kolkata, 700032

……
**Prof. Saswati Mazumdar**
Head of the Department of
Electrical Engineering
Jadavpur University
Kolkata, 700032

# Faculty of Engineering and Technology
# Jadavpur University, Kolkata - 700032

## Certificate of Approval

The forgoing thesis entitled "**Hybrid model of PMSG based WECS with PV array connected to the grid using back-to-back converter**" is hereby approved as a creditable study of an Engineering subject carried out and presented in a manner that fulfils its acceptance as a prerequisite to the degree for which it is submitted. It is understood that by this approval, the undersigned does not necessarily endorse or approve any statement made, opinion expressed, or conclusion drawn therein but approves the thesis only for the purpose for which it is submitted.

**The final examination for evaluation of the thesis**

Signature of the examiners

……

……

……

……

……

# Declaration of Originality

I hereby declare that this thesis contains a literature survey and original research work done by me. All the information in this document has been obtained and presented according to academic rules and ethical conduct. I also declare that, as required by these rules and conduct, I have fully cited and referenced all material and results that are not original to this work.

Name: Pritam Kumar

Examination Roll No: M4ELE22009

Thesis Title: Hybrid model of PMSG based WECS with PV array connected to the grid using back-to-back converter.

Signature with Date:

# ACKNOWLEDGMENT

I express my sincere gratitude to my supervisor**, Dr. Debashis Chatterjee** for his encouragement, suggestion and advices, without which it would not have been possible to complete my thesis successfully. I would like to thank **Prof. Nikhil Mondal and Prof. Mihir Hembram** for being a constant source of encouragement, inspiration and for their valuable suggestions coupled with their technical expertise throughout my research work. It was a great honour for me to pursue my research under his supervision.

I would also like to thank Mukul Anand, Rupali Mohanty research scholars of Drives lab, my co-workers and all the staffs of Drives and Simulation laboratory of our department for providing constant encouragement throughout my thesis work.

Last but not the least I extend my words of gratitude to my parents for personally motivating me to carry out the work smoothly.

# ABSTRACT

Renewable energy sources have become a popular alternative electrical energy source where power generation in conventional ways is not practical. In the last few years the photovoltaic and wind power generation have been increased significantly. Due to the rising use of wind energy, extensive research and analysis are required to determine how wind turbine generators affect the grid's quality of electricity. One of the potential technologies in wind power generating plans is the direct-driven permanent magnet synchronous generator (PMSG) with a back-to-back converter set. In this paper hybrid model of PMSG based WECS and PV array are used to analyze the power. A simple control technique which is also cost effective has been proposed to track the operating point at which maximum power can be coerced from the PV system and wind turbine generator system under continuously changing environmental conditions. The entire hybrid system is described given along with comprehensive simulation results that discover the feasibility of the system. A software simulation model is developed in Matlab/Simulink.

# ABBREVIATION AND ACRONYMS

| | |
|---|---|
| PV | Photo Voltaic |
| MPPT | Maximum Power Point Tracking |
| PMSG | Permanent Magnet Synchronous Generator |
| MSC | Machine Side Converter |
| GSC | Grid Side Converter |
| DC | Direct Current |
| P&O | Perturb and Observe |
| IC | Incremental Conductance |
| STC | Standard Test Condition |

## List of Symbols Used

| | |
|---|---|
| $I_{PV}$ | Photo voltaic current |
| $\alpha$ | Ideality factor |
| $V_T$ | Thermal voltage |
| $I_{pv\_STC}$ | Rated solar current at nominal weather ($25^0$C, 1000w/$m^2$ ) |
| $K_I$ | cell's short circuit current temperature coefficient |
| G | solar irradiance |
| $G_{STC}$ | Solar irradiance at nominal weather ($25^0$C, 1000w/$m^2$ ) |
| $I_{o\_STC}$ | Reverse saturation current of PV cell |
| $E_g$ | Band-gap energy of semiconductor material |
| ρ | air density (kg/$m^3$), |
| p | air pressure, |
| T | temperature on the absolute scale |
| R | gas constant. |
| r | Blade length (m), |
| $V_w$ | Wind speed (m/s), |
| $C_p$ | Power coefficient |
| λ | tip speed ratio |
| β | pitch angle |
| $L_q$ | Quadrature axis inductance |
| $L_d$ | Direct axis inductance |

# List of Figures

# Table of Contents

# Chapter 1

# Introduction

## 1.1 Motivation of the Work

Since carbon emissions are the primary driver of climate change, it is a serious worldwide problem that necessitates severe mitigation measures. For a more sustainable and clean environment, switching to renewable energy and low-carbon energy are implicit. Even though achieving carbon neutrality would necessitate considerable action by a wide range of companies and stakeholders, wind power, one of the fastest-growing renewable energy sources, is positioned to be a keystone in accelerating the global energy transformation. having a sizeable worldwide market share, the WECS based on doubly fed induction generators (DFIG) is a well-liked design for medium-size turbines.

However, a recent development is aimed towards taller and larger wind turbines, including model based on PMSG, to achieve maximum energy absorption through their related full-scale converter systems and extract more power. A comparison of DFIGs and PMSGs revealed that a PMSG had a failure rate throughout the early life of the machine that is 40% lesser when comparing with DFIG. Reactive power correction and a seamless grid connection are made possible by the system's full-scale converters and abilities to run at full speeds ranges.

## 1.2 Literature review

In the current global energy environment, power generation from renewable energy sources is becoming more and more significant. Fossil fuels are used to generate the majority of the energy. However, these fuels are very scarce, and conventional power generation techniques come with a host of environmental hazards. Solar photovoltaic (PV) and wind energy systems (WECS) are the most popular grid-connected renewable energy systems [1]. The solar radiation falling on the earth's surface is approximately 90 PW or 90xl012 Watt; thus, a small area use on the earth's surface can meet our electricity needs. Wind energy has the potential to generate enormous amounts of power, but its availability cannot be predicted. Solar power is available throughout the day, but the solar irradiance levels change due to changes in the sun's intensity and shadows caused by a variety of factors. Solar and wind energy are generally abundant in nature. As a result, the hybrid photovoltaic and wind energy system is more dependable in providing consistent power than either of them operating independently. Another advantage of hybrid systems is that the amount of battery storage can be reduced because hybrid systems are more reliable than independent systems. The amount of energy recovered from the wind is influenced by both the control system used on the wind energy conversion device and the incident wind speed. Typically, fully regulated variable speed wind turbine generators are used to extract the most wind energy possible. To follow the trajectory of the maximum wind power, the rotating speed of the wind turbine hub is modified in accordance with the incident wind speed [2]. A hybrid generating system uses many sources so that we can simultaneously harvest energy from several sources, increasing efficiency. The operation of the PV/Wind hybrid system, as well as the various topologies that can be employed to hybridize more than one system and the benefits and drawbacks of hybrid systems [2], [3]. Basic information about PV cells, PV modules, and PV arrays as well as their modelling is studied from [4] and [5]. Additionally, studies are done on how PV modules behave under various environmental conditions, such as solar radiation and temperature. The behavior of a PV module under partial shade conditions and ways to reduce its negative impacts are described in [6] - [8].

WECS typically use two power conversion stages, one at the generation end using an AC/DC machine-side converter (MSC) and the other at the grid side using a DC/AC grid-side converter (GSC). The size, price, and complexity of the system converter increase since PMSG MSCs are full-scale power converters that must be rated at the same level as the generator capacity. MSCs typically come in two types: active front-end converters or passive front-end converters (diode rectifier) that can benefit from boost DC/DC converter assistance. Passive front-end converter architecture can be a desirable approach in an effort to reduce the converter size and cost. It has fewer active switches, which results in fewer gate-drive circuits, which simplifies the installation and control of the converter. In addition, switching losses are lower, particularly at low and moderate turbine speed circumstances [7, 8]. Passive front-end converters are regarded as a popular option for low and medium power ranges as a result [9]. Due to the generator stator currents' uncontrollable character, utilizing this topology comes with a trade-off of larger torque ripples [7, 9, and 10].

Different MPPT techniques, their benefits and drawbacks, and the need for MPPT control [11]. From [13] to [17], the wind energy system's operation as well as methods for gaining the most electricity possible are explained. A research of the various types of bi-directional converters, how they operate, and how to use them for battery charging and discharging is conducted [18 - 20].

## Organization of the Thesis

This section presents an outline of the work carried by the author.

**Chapter-1** contains the motivation behind the work along with the review of different literature available on the above-mentioned topic and their limitations.

**Chapter-2** brief discussion on Photovoltaic energy system along with working principle and modelling of PV array, also describe MPPT and its types.

**Chapter-3** describe the Wind Power System and its power flow .this chapter also shows how power lost at different stages.

**Chapter-4** presents the PMSG based WECS modelling of wind turbine and modelling of PMSG also describe the machine side converter scheme and grid side converter scheme.

**Chapter-5** shows the MATLAB/Simulink model of this proposed scheme, results and discussion about modelling and its results.

**Chapter-6** contain conclusions and a possible future scope of work in this area.

# Chapter 2

# Photovoltaic Energy System

## History

Few materials, according to a theory first out in 1839 by French physicist Edmund Becquerel, are capable of generating electricity being exposed to sunlight. However, in 1905, Albert Einstein provided an explanation of the photoelectric effect and the nature of light. According to the photoelectric effect, when photons or sunshine touch a metal surface, an electron flow will occur. Later, the fundamental idea behind the technology of photovoltaic power generation was the photoelectric effect. Bell Laboratories produced the first photovoltaic module in 1954. Reduced costs and new opportunities for remote terrestrial application powering resulted from improvements in PV module manufacturing, performance, and quality in the 1970s. These opportunities included battery charging for navigational aids, signals, telecommunications equipment, and other crucial low-power requirements. In the 1980s, photovoltaic systems became a popular power source for consumer electronics including calculators, watches, radios, lanterns, and other compact battery-charging gadgets. Significant work was also put into developing PV power systems for home and commercial usage after the energy crises of the 1970s, both for stand-alone, remote power as well as for utility-connected applications. During this time frame, the number of worldwide applications for PV systems that power off-grid homes, rural health clinics, refrigeration, water pumping, and telecommunications expanded significantly.

## 2.1 Photovoltaic Arrangement

Solar technology known as photoelectric cells, or simply PV cells, turns light energy into electrical energy directly. In a photovoltaic cell, sunlight causes electrons to flow, for generating an electrical current.

The voltage level is adjusted by the dc-dc converter to correspond with the electrical appliances that are fed by Photovoltaic system. Depending on the required and available voltage levels, this DC-DC converter may be either buck, boost, or buck-boost. The maximum power point tracing system (MPPT) coerces the PV modules to produce their maximum power. When there is surplus of power, a bi-directional converter that can deliver current in both ways is used to charge the battery, and when there is a power deficit, the energy stored in the battery is discharged into the loads.

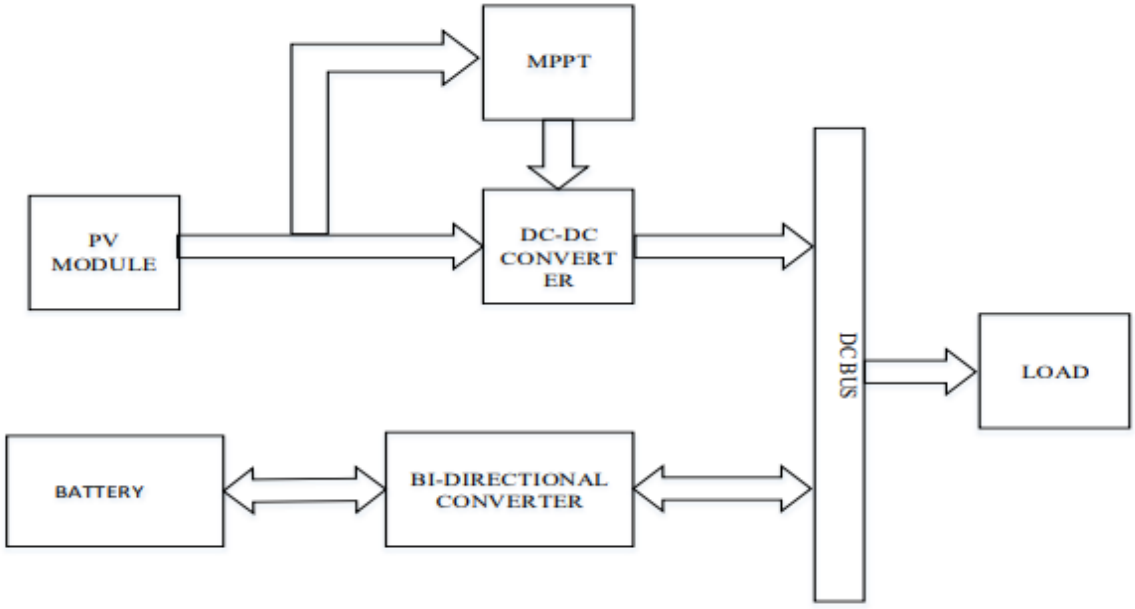


Fig.2.1 block diagram of PV energy system

### 2.1.1 PV Cell

When sunlight strikes on photovoltaic (PV) cell, also known as a solar cell, can either reflect, absorb, or pass through light that strikes it. The semiconductor material that makes up the PV cell can conduct electricity more effectively than an insulator but not as effectively as a good conductor like a metal. PV cells utilize a variety of semiconductor components.

When a semiconductor material is exposed to light, the light's energy is absorbed and transferred to the semiconductor's negatively charged electrons. The additional energy enables the electrons to conduct an electrical current through the material. This current can be used to power your home and the rest of the electric grid by extracting it through conductive metal contacts, which are the grid-like lines on solar cells.

A PV cell's efficiency can be calculated as the ratio of the electrical power it produces to the energy from the light shining on it. This ratio shows how well the cell converts energy from one form to another. The qualities of the available light (such as its intensity and wavelengths) and a number of cell performance factors determine how much power is generated by PV cells. The band gap, which describes what wavelengths of light the substance can absorb and convert to electrical energy, is a crucial features of PV semiconductors. The PV cell can efficiently use all of the available energy if the semiconductor's band gap matches the wavelengths of light shining on it.

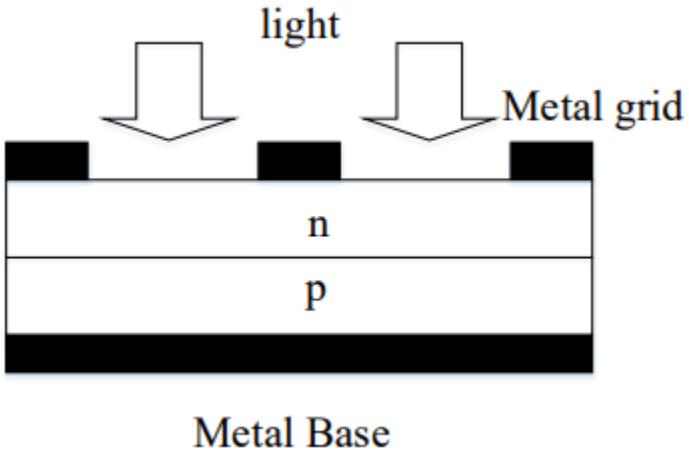


Fig 2.2 structure of PV CELL

### 2.1.2 PV Module

The useful output cannot be produced by a single solar cell. Therefore, it is necessary to Connect a number of these PV solar cells in order to boost the output power level of a PV system. A solar module typically has enough solar cells linked in series to produce the required standard output voltage and power. A single solar module can range in power from 3 to 300 watts. The fundamental component of a solar electric power generation system that is readily available on the market are solar modules, often known as PV modules.

Actually, only a very small amount—between 0.1 and 2 watts—is produced by a single solar PV cell. However, using such a low power unit as a system building block is not practicable. Therefore, the sufficient number of these cells are combined to create a useful, commercially available solar unit known as a solar module or PV module.

### 2.1.3 PV Array

A photovoltaic array is nothing more than the serial or parallel interconnection of several PV modules. Individual modules might not be able to produce enough power to satisfy the needs of trading applications, so the modules are secured in a grid or as an array to meet the load requirements. In an array, the modules are connected similarly to how a module's cells are connected. When building a PV array, the modules are often first connected in serial fashion to achieve the necessary voltage, and then the strings so produced are joined in parallel to provide more current as needed.

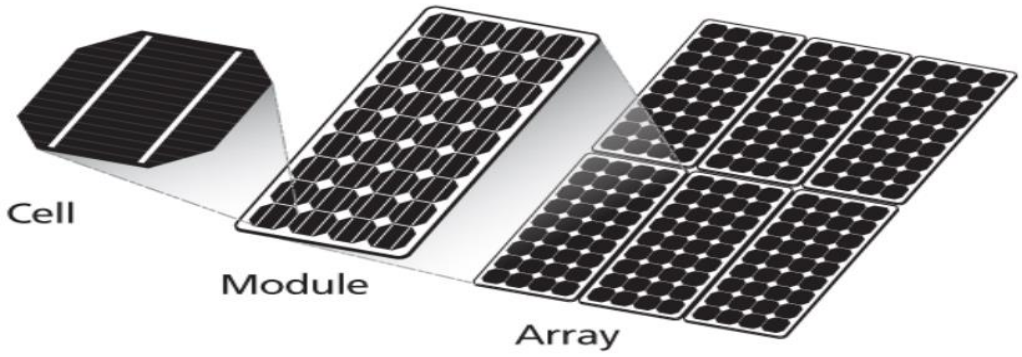


Fig 2.3 Photovoltaic system

## 2.2. Array Design

The major factors influencing the electrical design of the solar array are as follows:

i. sun intensity
ii. sun angle
iii. load matching for maximum power
iv. Operating temperature

These factors are discussed in the following subsections

### 2.2.1 Sun Intensity

Under a full, shining sun, the photocurrent's magnitude is maximum (1.0 sun).The photocurrent decreases in direct proportion to the sun's intensity on a partly sunny day. The I-V characteristic shifts downward at reduced solar intensity. Therefore, the short-circuit current dramatically lowers during cloudy days. However, the open-circuit voltage is only slightly reduced. In the practical operating range, solar radiation has little effect on the cell's efficiency of photo conversion. The efficiency, for instance, is nearly the same at 500 $^{W}/_{m^2}$ and 1000$^{W}/_{m^2}$. This indicates that a sunny day's conversion efficiency is the same as one with clouds. On a cloudy day, we only produce slightly less power because to the reduced solar energy that strikes the cell.

### 2.2.2 Sun Angle

The output current of PV cell is given by

$$I = I_0 \cos\theta \tag{2.1}$$

Where, $I_o$ = current with normal sun (reference), and θ = angle of the sun line measured from the normal. The range of 0 to around 50° for the sun angle is well covered by this cosine law. Although the mathematical cosine law predicts 7.5 percent power generation, the electrical output deviates dramatically from the cosine rule beyond 50° and the cell produces no power beyond 85°. The Kelly cosine, which represents the PV cell's real power-angle curve.

### 2.2.3 Shadow Effect

A large number of parallel strings of cells connected in series could make up the array. A structure that interferes with the sun's line of sight could cause a big array to be partially shaded. A cell in a long series string that is totally in the shade loses the photo-voltage but still required to carry the string current because it is connected to all other cells that are still in the sun. The shadow of cell cannot be generated electricity without internally produced voltage. Instead, it serves as a load, causing heat and $I^2R$ loss locally. To make up for the voltage loss of the shaded cell, the remaining cells in the string must be operated at a greater voltage. According to the I-V characteristic of the string, a higher voltage of healthy cells results for lower string current. For a light shadow on a small region, the current loss is not proportional to the shadowed area and might not be observed. The I-V curve dips below the string's operational voltage as additional cells are shadowed beyond the critical threshold, causing this string current to fall to zero and the string's whole power to be lost. One complete string is lost from the array as a result of this. Divide the circuit length into many parts using bypass diodes is a frequent technique for reducing losses of string power caused by a potential shadow. Only that portion of the string is avoided by the diode crossing over the

shaded segment. Without affecting the power of the entire string, this results in a relative loss in string voltage and current. Some contemporary PV modules include such inbuilt bypass diodes.

### 2.2.4 Temperature Effects

The cell's short-circuit current increases with temperature while the open-circuit voltage falls. By analyzing the consequences on the current and voltage individually, the influence of temperature on PV power is quantitatively assessed. Assume that at the reference temperature T, Io and Vo represent short-circuit current and open-circuit voltage respectively, and α, β are their temperature coefficients respectively. When operating temperature is risen by ΔT, then the new current and voltage will be given by the following equation:

$$I_{SC} = I_0(1 + \alpha \cdot \Delta T) \tag{2.2}$$

And,
$$V_{OC} = V_0(1 - \beta \Delta T) \tag{2.3}$$

## 2.3. Working of PV Cell

Although it has a somewhat different design from standard p-n junction diodes, a solar cell is fundamentally a junction diode. On top of a somewhat thicker n-type semiconductor, a very thin layer of p-type semiconductor is formed. Next, we add a few smaller electrodes to the p-type semiconductor layer's top. These electrodes don't prevent light from passing through to the thin p-type layer. A p-n junction is located just beneath the p-type layer. A current-collecting electrode is additionally provided at the base of the n-type layer. To shield the solar cell from any mechanical disturbance, we encase the complete device in a thin glass shell.

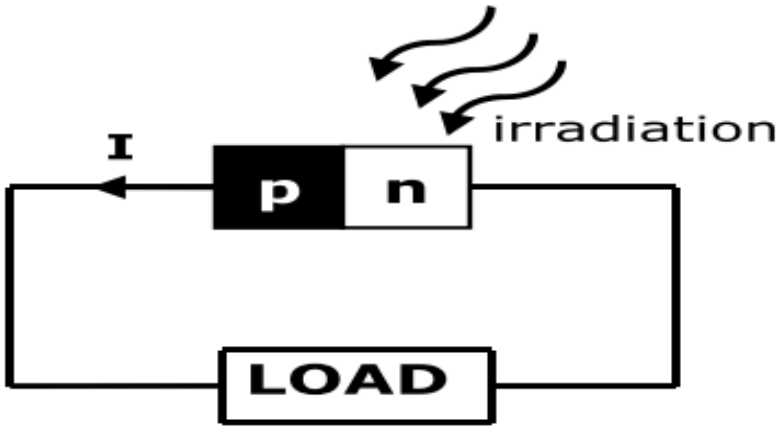


Fig.2.4 working of PV Cell

Light photons easily pass through the very thin p-type layer at the p-n junction when it comes into contact with it. The photons give the junction enough energy to make multiple electron-hole pairs. The junction's thermal equilibrium condition is broken by the incident light. The depletion region's free electrons can move quickly to the junction's n-type side. Similarly, depletion holes can quickly reach the p-type side of the junction. Because of barrier potential of the junction, newly created free electrons cannot cross the junction once they reached the n-type side.

Similarly, newly formed holes cannot cross the junction once they reach the p-type side because they have the same barrier potential as the junction. The p-n junction will act like a miniature battery cell as one side of the junction, the n-type side, experiences higher electron concentrations and the other side, the p-type side, experiences higher hole concentrations. A voltage known as the photo voltage is set up. A minor current will flow across the junction if we attach a small load across it.

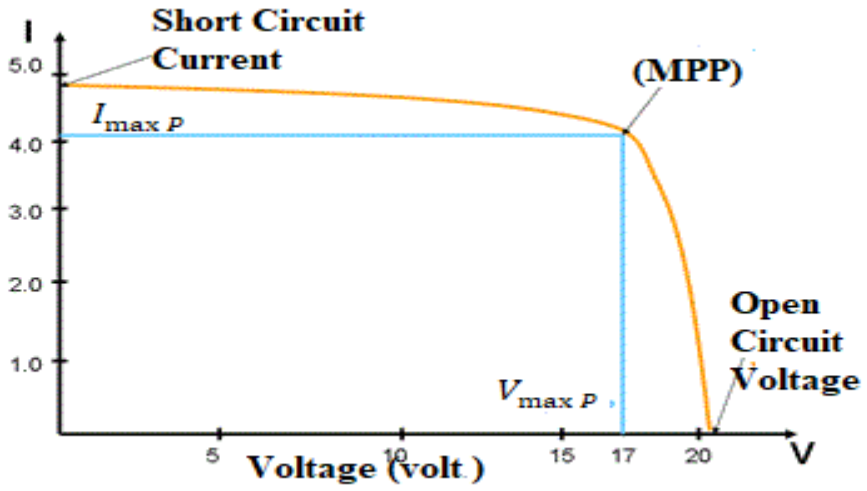


Fig.2.5 I-V characteristics of PV Cell

## 2.4. Modelling of PV Cell

The three main points of interest for any PV cell are as follows:

The short-circuit (SC) condition is recognized by a zero voltage at the terminal of PV module and by the short-circuit current (Isc).

A zero current in the PV panel terminals and an open-circuit voltage (Voc) are the two characteristics of the open-circuit (OC) situation.

The PV panel can generate the maximum power under temporary working conditions at the MPP, where the current value is$I_{MPP}$, the voltage value is$V_{MPP}$, and the power

$$P_{MPP} = I_{MPP} \times V_{MPP} . \quad (2.4)$$

### 2.4.1 Mathematical Model of SPV Cell

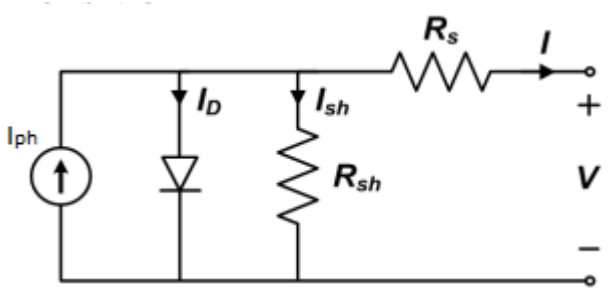


Fig 2.6 Equivalent circuit solar cell

This above figure represents the practical model of single solar cell. Where, series resistance of PN junction cell is represented by $R_S$ and $R_{Sh}$ represents shunt resistance which has an inverse relationship with leakage current to ground. On V-I characteristics series resistor put a great impact $I_D$ and $I_{sh}$ are the diode current and shunt leakage current, the output terminal current I can be calculated by applying KCL in this circuit diagram;

$$I = I_{ph} - (I_d + I_{sh}) \tag{2.5}$$

Because photon current is generated when a solar cell absorbs solar radiation, photocurrent value is directly related to variations in solar irradiance and temperature and that is;

$$I_{PV} = \left(I_{PV\_STC} + K_I \Delta T\right) \frac{G}{G_{STC}} \tag{2.6}$$

Where,

$I_{pv\_STC}$ =rated solar current at nominal weather ($25^0$C, 1000w/$m^2$ ),

$K_I$ = cell's short circuit current temperature coefficient,

G = solar irradiance;

$G_{STC}$ = solar irradiance at nominal weather ($25^0$C, 1000w/$m^2$ ),

ΔT = difference between operating and nominal temperature.

Whereas, the reverse saturation current of a solar cell will be calculated by;

$$I_o = I_{o\_STC}\left(\frac{T_{STC}}{T}\right)^3 exp\left[\frac{qE_g}{\alpha K}\left(\frac{1}{T_{STC}} - \frac{1}{T}\right)\right] \quad (2.7)$$

Where, $I_{o\_STC}$ reverse saturation current of PV cell at nominal temperature and irradiance values and $E_g$ represents band-gap energy of semiconductor material.

As a function of temperature, the reverse saturation current can be further enhanced as shown below;

$$I_o = \frac{\left(I_{SC\_STC} + K_I \Delta T\right)}{exp\left[\frac{\left(V_{OC\_STC} + K_V \Delta T\right)}{\alpha V_T}\right] - 1} \quad (2.8)$$

Where, $I_{SC\_STC}$ and, $V_{SC\_STC}$ are the short circuit current and open circuit voltage at nominal weather condition ($25^0$C, 1000w/$m^2$ ),

Many authors recommend more sophisticated models for greater accuracy and for other objectives. The result of the recombination of carriers is depicted in some models by an additional diode. Some authors additionally employed three-diode models that include influences of various additional variables not before taken into account. However, to keep things simple, we employ a single diode model for our work.

As $R_{Sh}$ of the PV cell is inversely proportional to the shunt leakage current to ground, it can be assumed that it will be very large value for a very small leakage current to ground. The efficiency of a PV cell does not depend on the variation in the shunt resistance $R_{sh}$of the cell, but efficiency of a PV cell greatly depends on the variations in series resistance$R_S$. In order to meet our desired need, we used a combination of PV cells because the total power generated by a single PV cell is relatively low. The term "PV array" refers to this grid of solar cells. If $N_P$ represents parallel cells and $N_S$ represents series cells then the PV array's equations can be expressed as;

$$\mathrm{I} = I_{PV}N_P - I_O N_P\left[exp\left(\frac{V + IR_S\left(\frac{N_S}{N_P}\right)}{\alpha V_T N_S}\right) - 1\right] - \left(\frac{V + IR_S\left(\frac{N_S}{N_P}\right)}{R_P\left(\frac{N_S}{N_P}\right)}\right) \quad (2.9)$$

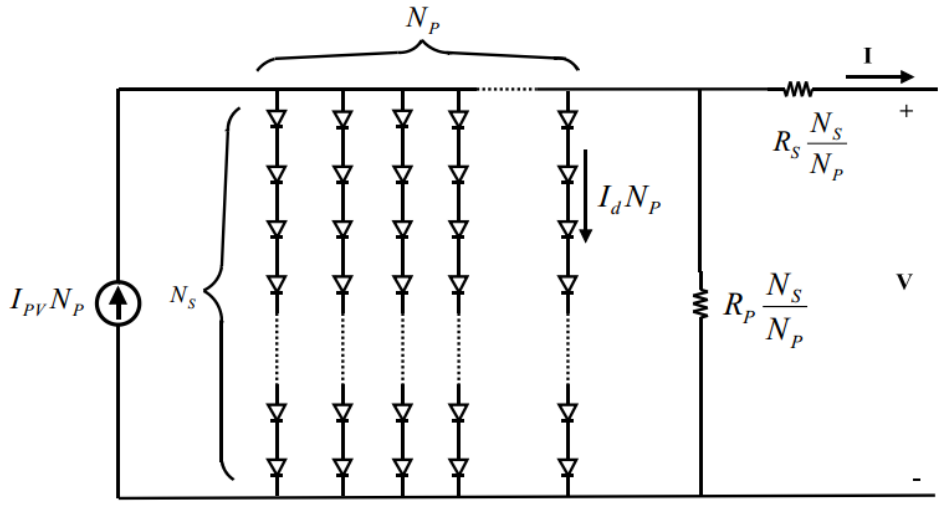


Fig .2.7 PV Cell equivalent diagram

PV cell efficiency can be more significantly impacted by a modest variation in series resistance than by a variation in shunt resistance. Shunt resistance should be infinite and can be viewed as open for extremely low leakage currents to ground. After taking shunt resistance to infinite, the mathematical equation of this model can be written as:

$$\mathrm{I} = I_{PV} N_P - I_O N_P \left[ exp\left( \frac{V + IR_S\left(\frac{N_S}{N_P}\right)}{\alpha V_T N_S} \right) - 1 \right] \tag{2.10}$$

The two main parameters that are used to relate the electrical performance are the PV cell open-circuit voltage $V_{OC}$ and short- circuit current $I_{SC}$ .

The maximum power can be calculated as-

$$P_{max} = V_{max} . I_{max} \tag{2.11}$$

## 2.5. Maximum Power Point Tracking

MPPT, or Maximum Power Point Tracking, is a charge controller algorithm that is used to extract the maximum available power from a PV module under certain conditions. The maximum power point is the voltage at which a PV module can produce the max power (or peak power voltage). Maximum power is affected by solar radiation, ambient temperature, and the temperature of the solar cell. The MPPT control system is an entirely electronic system that can produce the maximum permissible power by changing the electrical operating point of the modules.

### 2.5.1 Necessity of Maximum Power Point Tracking

The maximum power voltage of a typical PV module is approximately 17 V when measured at a temperature of 25 C of the cell. On extremely hot or extremely cold days, this voltage can fluctuate between 15 and 18 V. The main goal of MPPT is to get the most power possible out of PV modules by operating them at the highest effective voltage.

The MPPT algorithm is based on the straight forward idea for calculation of the output of a PV module, compares it to the battery voltage, and then determines the maximum power that a PV module can generate to charge a battery. Then it converts that power to the best possible voltage to deliver the maximum amount of current into the battery. Additionally, it has the ability to power up a DC load that is linked directly to the battery. Cloudy days and fully depleted batteries are the best times to use MPPT.

### 2.5.2MPPT algorithm

There are many algorithms which help in tracing the maximum power point of the PV module. They are following:

a. P&O algorithm (hill climbing method)

b. IC algorithm (Incremental Conductance method)

c. Parasitic capacitance algorithm

d. Voltage based peak power tracking algorithm

e. Current based peak power tracking algorithm

## Perturb and observe

The P&O method's implementation costs are lower since only one voltage sensor is required to measure the PV array's voltage. The algorithm requires changing both the operating voltage of the DC-link connecting the PV array and the power converter as well as the duty cycle of the power converter. Modifying the power converter's duty cycle entails changing the DC-link voltage between the PV array and the power converter. The next perturbation in this method is determined by the sign of the most recent perturbation and the most recent power increment.

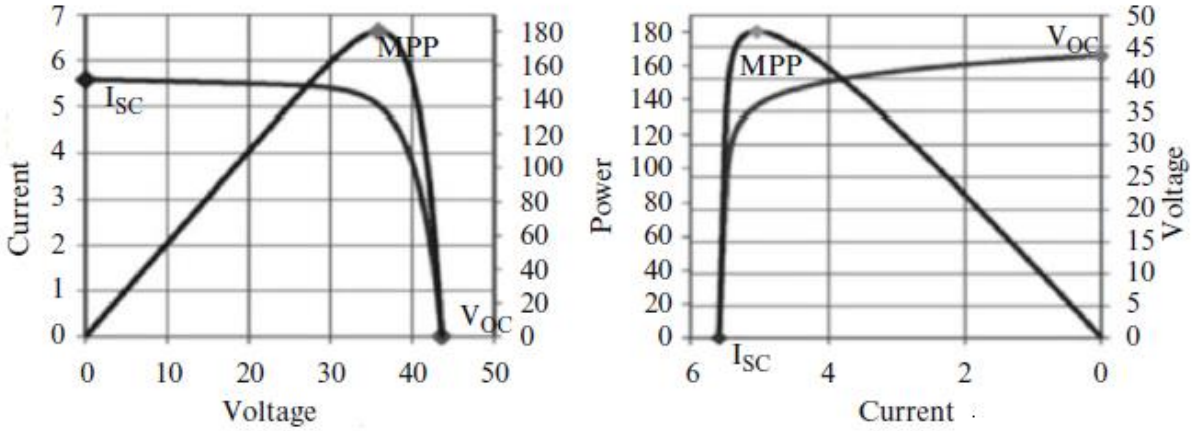


Fig.2.8 PV characteristics curve

As we can see from the above figures, increasing the voltage on the left of the MPP increases the power, while decreasing the voltage on the right decreases the power. The next perturbation should be in the other direction if the power falls, and the perturbation should remain in the same direction if the power increases. This algorithm is implemented as shown in the flowchart based on these facts.

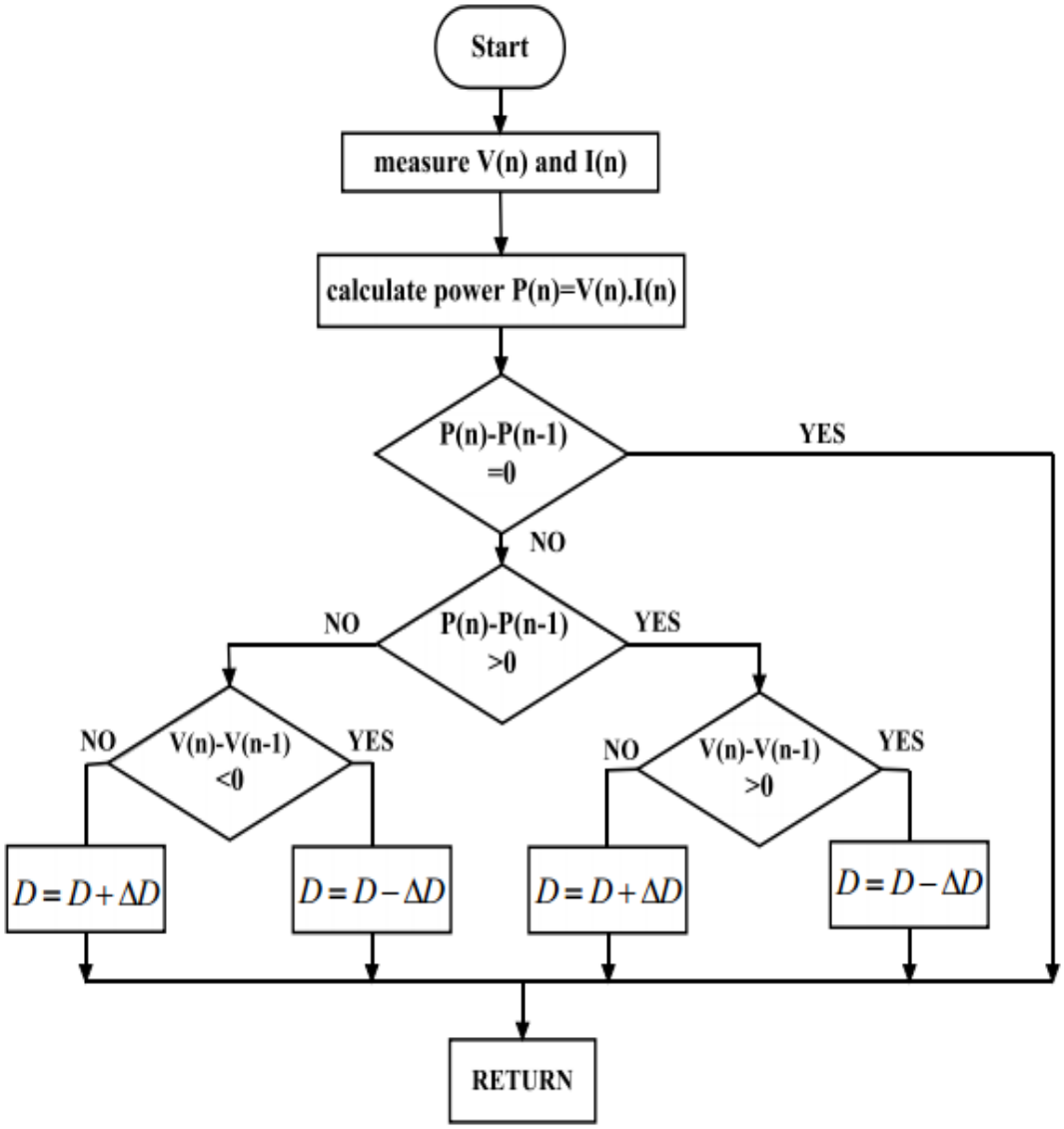


Fig.2.9 flowchart of perturb and observe algorithm

As shown in the flow chart, we first measure voltage and current, then calculate power using these values. The calculated power is then compared to the previous one, and we adjust the voltage to find the Maximum Power Point by adjusting the duty cycle of the converter.

# Chapter 3

# Wind Power System

## History

Wind power was used for sailing ships on the Nile for the first time around 5000 years back. Many civilizations have employed wind power for transportation and other purposes. In the late 1700s and early 1800s, the Europeans used it for pumping water and grinding wheat. For the purpose of generating energy in rural America, the first windmill was set up in 1890.

With an eye on the nation's energy security, the Department of Non-Conventional Energy Sources was established in India in the 1980s with the goal of reducing our reliance on primary energy sources like coal and oil. The usage of wind energy is proving to be the most efficient way to combat issues like the depletion of fossil resources, the importation of coal, greenhouse gas emissions, and environmental pollution in India. Green and clean electricity can be produced using wind energy, a renewable, non-polluting, and cost-effective source. Renewable energy sources (excluding large hydro) currently account for 27.78 percent of total installed power capacity of India with a total installed capacity of 40358MW (March 2022) of wind energy. The majority of renewable energy capacity is held by wind energy at 36.73 percent which is still a key source of clean energy.

The Indian government has set a target for renewable energy of 175 GW by 2022, of which 60 GW will come from wind energy. Additionally, unlike all other power sources, wind energy doesn't use any water, which is already a rare resource. In India, wind energy has a promising future as a source of energy security. The primary benefit of wind energy is that it is emission-free and has no cost for the fuel. When compared to other renewable

energy sources, wind farms are more affordable, can be erected quickly, and can be utilized for farming as well.

## 3.1 Wind Turbine

In order to generate electricity, a wind turbine used to convert the kinetic energy of the wind into spinning mechanical power for the turbine rotor blades. To harness wind energy, the turbine is mounted on a tall tower. To create a wind farm with the appropriate power generation capacity, several wind turbines are installed at one location.

Two different types of configurations for turbine design:

i. The horizontal-axis configuration wind turbine
ii. The vertical-axis configuration wind turbine

The horizontal axis configuration is frequently referred to as a Danish wind turbine. The machine with a vertical axis configuration resembles an egg beater and is occasionally referred to as the Darrieu's rotor after its creator. In the past, the vertical-axis arrangement was used due to its unique structural advantages. Today's wind turbines, however, have a horizontal axis design. The rotor is the only component that differs between the two designs; the majority of the other parts are identical.

## 3.2 Power flow of Wind Turbine System

The power flow from the wind turbine to the power accessible to the grid must be analyzed in order to comprehend all losses in the Wind Turbine System (WTS).

Three stages can be used to group all losses.-

First stage: Wind capture losses and severe friction losses; from wind power to the generator.

Second stage: Generator losses; from input shaft power to rectifier.

Third stage: Frequency converter losses; from power available to rectifier to power produced at the grid.

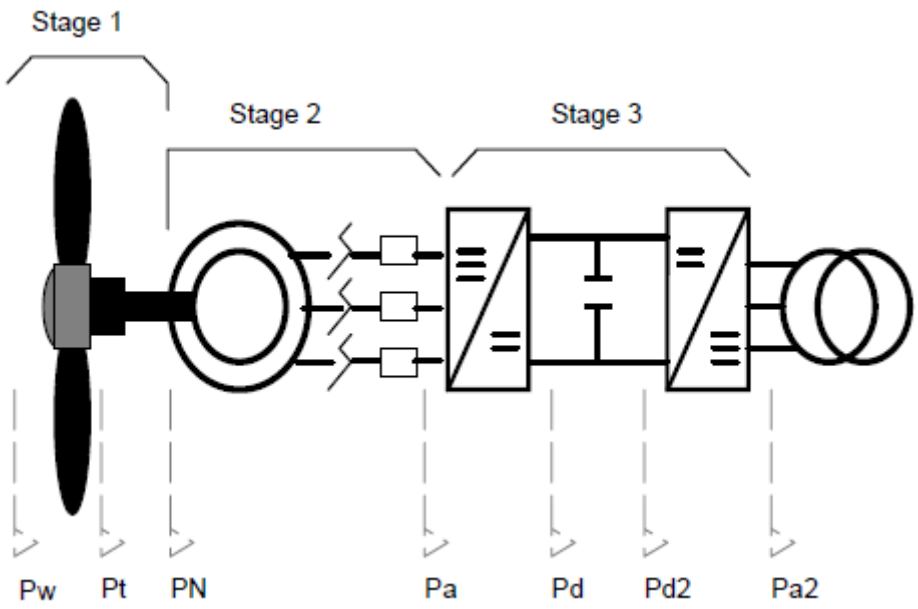


Fig .3.1 Wind Turbine model

**First Stage**

The kinetic energy in wind of mass m, flowing at velocity V, in x direction is,

$$K.E = \frac{1}{2}(\rho Ax)V^2 \quad \text{Joule} \tag{3.1}$$

According to Betz' law, the wind power that the wind turbine can capture is

$$P_t(v) = C_P(v, n)\frac{1}{2}\rho_a A_t v^3 \tag{3.2}$$

**Second stage**

In this stage individual losses of permanent magnet synchronous generator are considered.

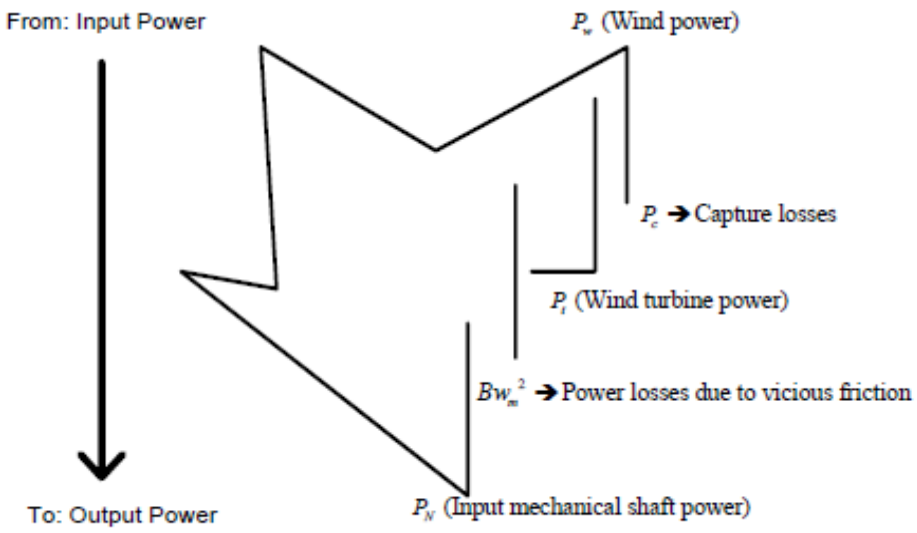


Fig .3.2 Power flow in First stage

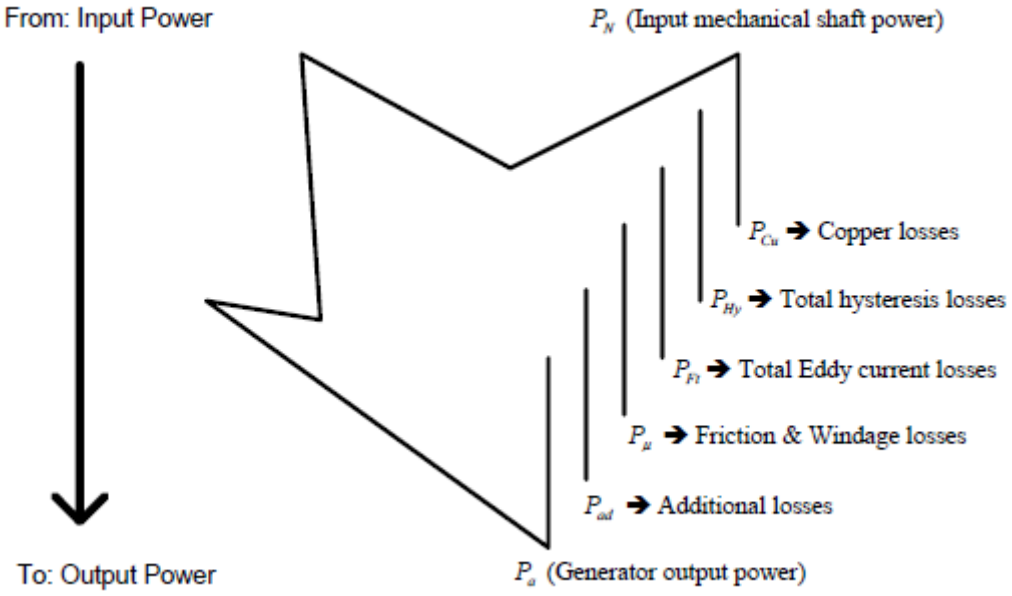


Fig .3.3 Power flow in Second stage

**Third stage**

Power from the generator is fed through an IGBT-based back-to-back converter. A MSC (machine side converter), a dc link capacitor, and a GSC make up the converter (grid side converter). MSC transfers the voltage from AC to DC by acting as a rectifier. The rectifier enables the generator to

run at a variable voltage and speed to enhance wind turbine energy extraction. GSC functions as an inverter, converting the dc link voltage Vdc into AC and supplying the grid with AC voltage and current. Since the back-to-back converter uses an IGBT gate. As IGBT operate at high frequency and result in considerable losses, switching losses are

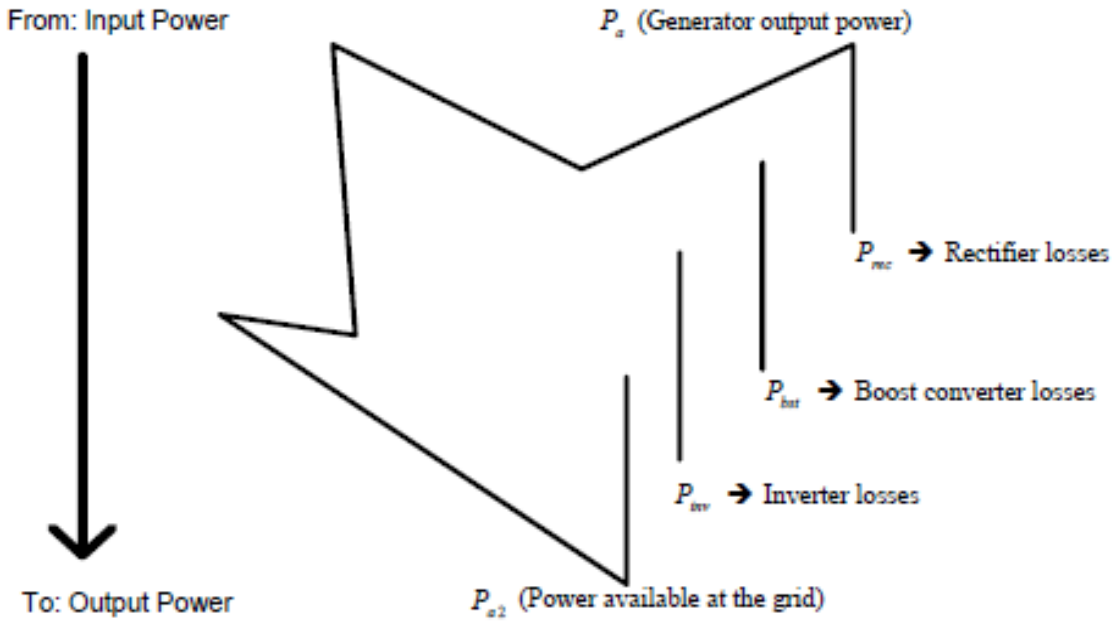


Fig .3.4 Power flow in Third stage

## 3.3 Speed and Power relations

The power in the moving air is flow rate of the kinetic energy per second in watts:

$$\text{Power} = \frac{1}{2}(\text{mass flow per second})\, V^2 \qquad (3.3)$$

If

P = mechanical power in the moving air (watts),

ρ = air density (kg/m$^3$),

A = area swept by the rotor blades (m$^2$),

V = velocity of the air (m/sec),

Then, Volumetric flow rate =AV, (3.4)

The mass flow rate of the air = ρAV, (3.5)

The mechanical power coming in the upstream wind is given by the following in watt.

$$P = \frac{1}{2}(\rho AV)V^2 = \frac{1}{2}(\rho AV^{3)} \quad (3.6)$$

This power is calculated in the upstream wind. It varies linearly with the density of the air sweeping the blades and with the cube of the wind speed (V). The blades cannot extract all of the upstream wind power, as some power is left in the downstream air that continues to move with reduced speed.

## 3.4 Power Extracted from the wind

The difference between the upstream and downstream wind powers is the real power that is extracted by the rotor blades.

$$P_0 = \frac{1}{2}(\text{mass flow per second})\,(V^2 - V_o^2) \quad (3.7)$$

Where,

Po = the mechanical power generated by the rotor, or the output power of the turbine

V = speed of the upstream wind at the rotor blades' entry, and

Vo = downstream wind speed at the rotor blades' exit.

At the "plane" of the rotor blades, the air velocity discontinuously changes from V to Vo, with an "average" of ½(V + Vo). . In order to determine the mass flow rate of air through the rotating blades, multiply the air density by the average velocity as shown below;

$$\text{Mass rate flow} = \rho A\frac{V + Vo}{2} \quad (3.8)$$

The mechanical power extracted by the rotor, which drives the electrical generator, is therefore

$$P = \frac{1}{4}(\rho AV^{2)}\left[1 + \frac{V0}{V}\right]\left[1 + \left(\frac{V0}{V}\right)\right] \quad (3.9)$$

Typically, a proportion of the upstream wind power, measured in watts, is used to indicate the power extracted by the blades. The percentage of upstream wind energy that is captured by the rotor blades and delivered to the electrical generator is known as Cp. The downstream breeze dissipates the remaining energy. The rotor's power coefficient or efficiency is another name for the quantity Cp.

The relationship between the downstream and upstream wind speeds (Vo/V), for a particular upstream wind speed, determines the value of Cp. The power vs. (Vo/V) plot demonstrates that Cp is a function with a single maximum value. When the Vo/V ratio is one-third, the value reaches its maximum of 0.59. At that speed ratio, or when the downstream wind speed is equal to one third of the upstream wind speed, the wind's maximum power is extracted. In this circumstance (in watts):

$$P_{max} = \frac{1}{2}(\rho A V^3) \times (0.59) \tag{3.10}$$

The greatest possible value of Cp is 0.59. The rotor tip-speed ratio (TSR) is frequently used to express Cp. The TSR is the ratio of the rotor's outermost tip's linear speed to the upstream wind speed. The relationship between the rotor tip speed and the wind speed is established by an aerodynamic analysis of the wind flow around a moving blade with a specified pitch angle. For modern, high-speed, two-blade turbines, the highest attainable Cp in realistic designs ranges between 0.4 and 0.5, and between 0.2 and 0.4 for slow-speed turbines with multiple blades. The maximum power output of the wind turbine is a straightforward expression if we use 0.5 as the practical maximum rotor efficiency (in watts per square meter of swept area).

## 3.5 Rotor swept Area

The rotor-swept area and the wind turbine's output power changes linearly. The rotor-swept area of the horizontal-axis turbine is as follows:

$$A = \frac{\pi}{4}D^2 \tag{3.11}$$

Where,

D = rotor diameter.

Determining the swept area for the Darrieus vertical-axis machine requires complicated work because elliptical integrals are involved. However, using a parabola to approximate the blade form results in the following straightforward expression for the swept area.

$A = \frac{2}{3}$(maximum rotor width at the Centre) (height of the rotor) (3.12)

Despite having only two or three thin blades with a solidity between 5-10 percent, the wind turbine successfully captures the wind energy flowing through the full swept area. The ratio of the solid area to the swept area of the blades is known as the solidity. The solidity ratio of the contemporary two-blade turbine is low. Because it uses low blade material to sweep wide areas, it is more cost-effective.

## 3.6 Air Density

Along with air density, wind power varies linearly as it passes over the blades. According to the gas law, the air density ρ varies with pressure and temperature:

$$\rho = \frac{p}{RT} \quad (3.13)$$

p = air pressure,

T = temperature on the absolute scale

R = gas constant.

At 1 atm and 60°F, the air density at sea level is 1.225 kg/m3. Using this as a guide, ρ is corrected for the site-specific temperature and pressure. Altitude affects both the temperature and the pressure. The following calculation, which is accurate up to 6,000 meters (20,000 feet) of site elevation above sea level, describes their combined impact on the air density:

$$\rho = \rho_0 e^{\frac{-0.029H}{3048}} \quad (3.14)$$

Where; H is the site elevation in meters.

The air density correction at high elevations can be significant. For example, the air density at 2100-m elevation would be 0.986 kg/m$^3$, 20% lower than the 1.225 kg/m$^3$ value at sea level. For ready reference, the temperature varies with the elevation as follows in °C:

# Chapter 4

# PMSG based grid connected WECS

Because PMSGs (Permanent Magnet Synchronous Generator) are self-excited and permit operation at high power factor and the efficiency, they are regarded as relevant and practicable technology in the wind generation business. Additionally, in contrast to other WECSs, the gearbox can be omitted due to its low rotational speed, where it is one of the most crucial turbine components and requires careful and routine maintenance because failure is widely anticipated.

Here, we'll discuss how grid-connected, directly-driven wind turbines built on the PMSG in continuous operation. The point of common coupling (PCC), uses a (ac-dc-ac) back-to-back converter set where the PMSG is linked to the grid. For converters on the grid side and in generator side, two control methods are proposed. The control strategy for the grid side converter is designed to operate at unity power factor and maintain the dc link voltage at its set-point., while control of the generator's side converter is developed to accomplish maximum power point tracking (MPPT).

## 4.1 System modeling

The rotor blades of wind turbines convert kinetic energy of the wind to the mechanical energy. The generator then converts the mechanical energy into electrical energy, which is transmitted to the grid via power converters.

Two primary components of the WECS under consideration are shown in Fig.4.1:

(a) Mechanical components, they comprise the drive train system and the aerodynamic system with the rotor blades (if existed).

(b) Electrical components, which include the back-to-back converter set and the PMSG.

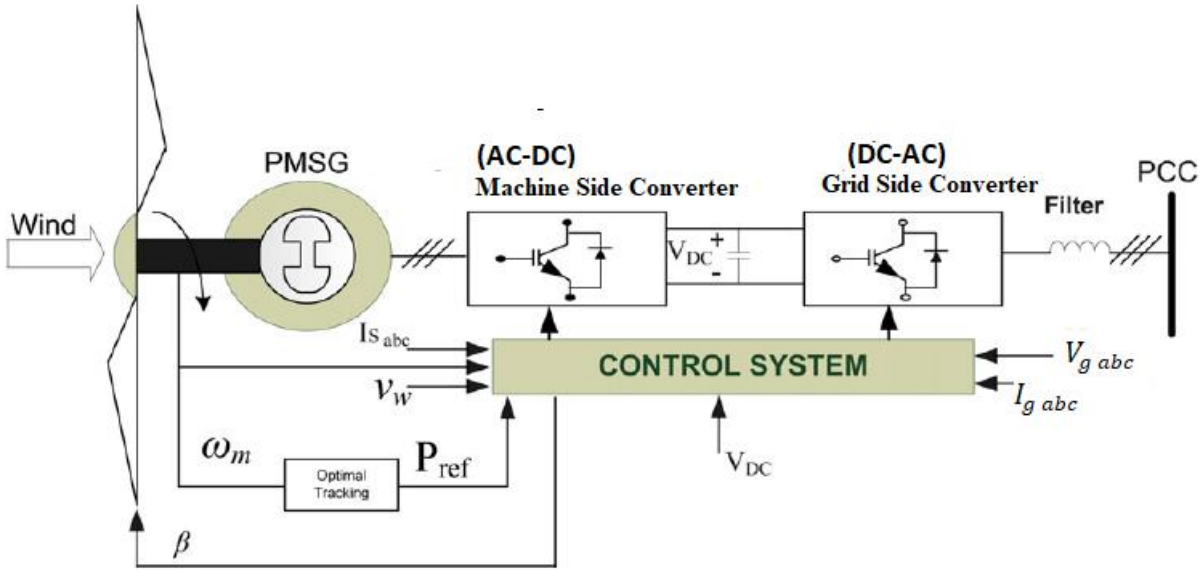


Fig .4.1 Wind Turbine configuration based on PMSG

### 4.1.1Mechanical parts representation

The mechanical part is in charge of converting the wind energy incident on the revolving turbine blades, with swept-area (A= $\pi r^2$) into the mechanical power. Mechanical power$P_m$;

$$P_m = \frac{1}{2} C_p \pi r^2 \rho V_w^3 \qquad (4.1)$$

Where, ρ= Air density ($^{kg}/_{m^3}$)

r = Blade length (m),

$V_w$ = Wind speed (m/s),

$C_p$ = Power coefficient,

The tip speed ratio (λ) and the blades pitch angle (β) affect the value of $C_p$. Depending on the model and condition of operation of the wind turbine, the integrated pitch controllers adjust the pitch angle of the blades. The formula for $C_p$ in mathematics is given as;

$$C_p = c_1 \left(\frac{c_2}{\lambda_i} - c_3\,\beta - c_4\right) e^{\frac{-c_5}{\lambda_i}} + c_6\lambda \tag{4.2}$$

$\lambda_i$ And $c_1$ - $c_6$ are discussed in Appendix

$$\text{Tip speed ratio } (\lambda) = \frac{w_t\, r}{V_w} \tag{4.3}$$

Where, $w_t$ = Rotational speed of the turbine shaft.

The mechanical input torque ($T_m$);

$$T_m = \frac{P_m}{w_t} \quad ; \tag{4.4}$$

As shown below in Fig.4.2, Three states of operation can be distinguished in the working zone of wind turbines: standstill, normal condition, and pitched condition...

The wind power is insufficient to drive the wind turbine's rotor because of friction and inertia of turbine. At the end boundary of the standstill region, where the cut-in speed is shown, the turbine starts to run. The cut-in wind speed used in this study is 3 m/s, or $w_t$ = 12.15 rad/s.

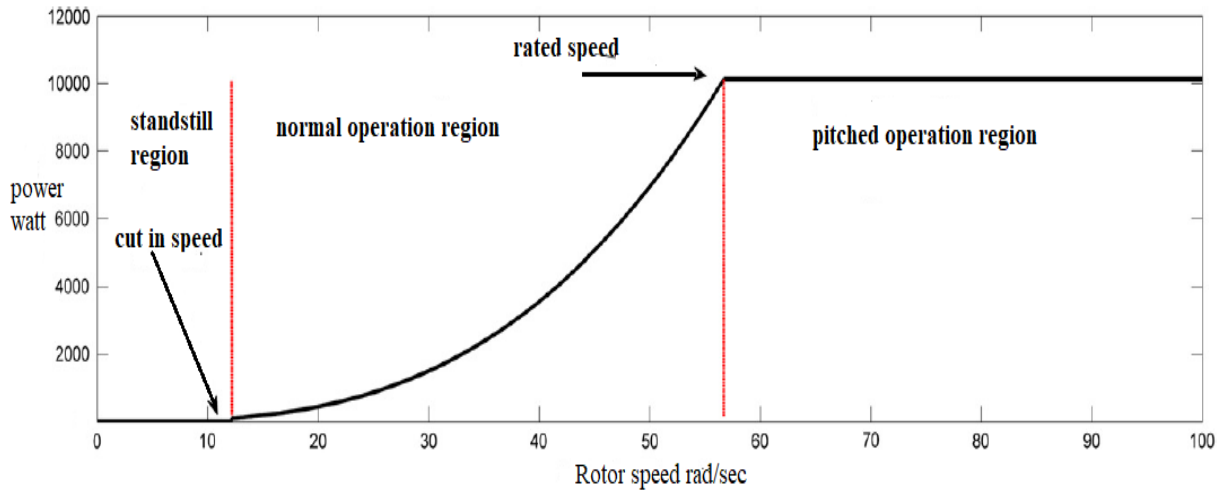


Fig .4.2 operational scheme of turbine.

In order to implement the MPPT strategy, the wind turbine should be run at maximum $C_p$ with a fixed pitch angle, β = 0, in the normal operation condition.

$C_p - \lambda$ Family of curves is shown in Fig.4.3 for various pitch angles, with the power coefficient's maximum value, $C_{p\_max}$ ≈0.48, given at β = 0 and λ = λoptimum ≈ 8.1. When the normal zone terminates, as shown in Fig. 4, the wind speed reaches its rated value of 14 m/s, which is nearly equal to$w_t = 56.7\, rad/s$, the maximum amount of power may be captured at the optimum rotating speed for any particular wind speed.

Last but not least, the pitch control system limits the power that the blades can capture in the region of pitched operation. The power produced by the wind turbine increases together with the wind speed. When the turbine power rating is reached, the pitch angle needs to be increased to lose the aerodynamic power (shown by the rated wind speed). As the pitch angle rises, the wind turbine's efficiency declines.

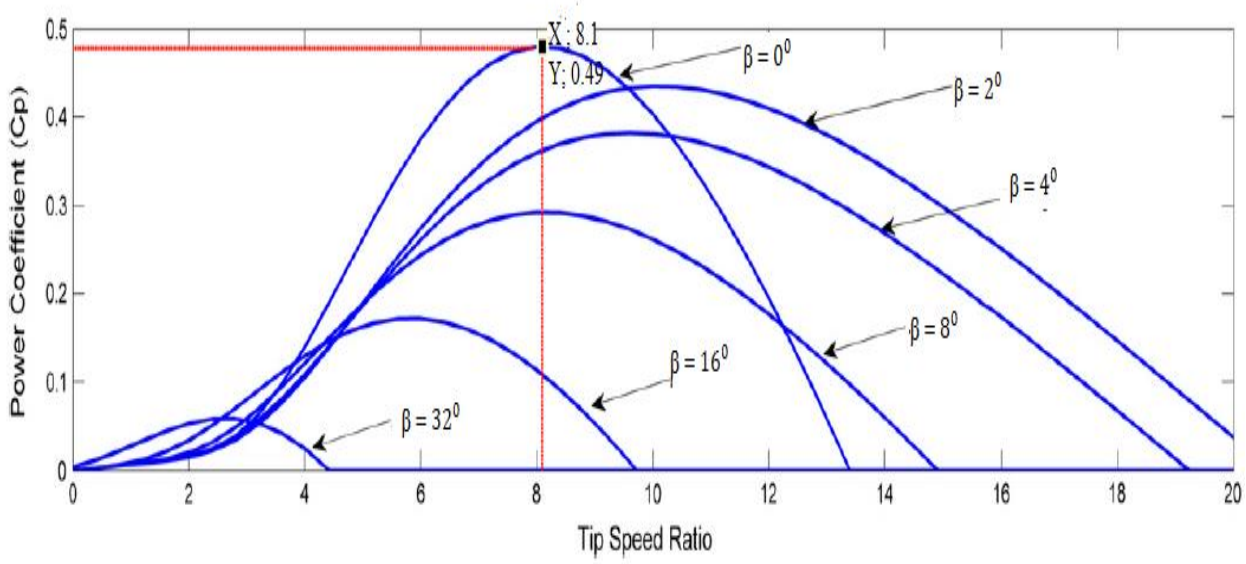


Fig.4.3 $C_p v/s\ \lambda$ curves for the different pitch angle (β)

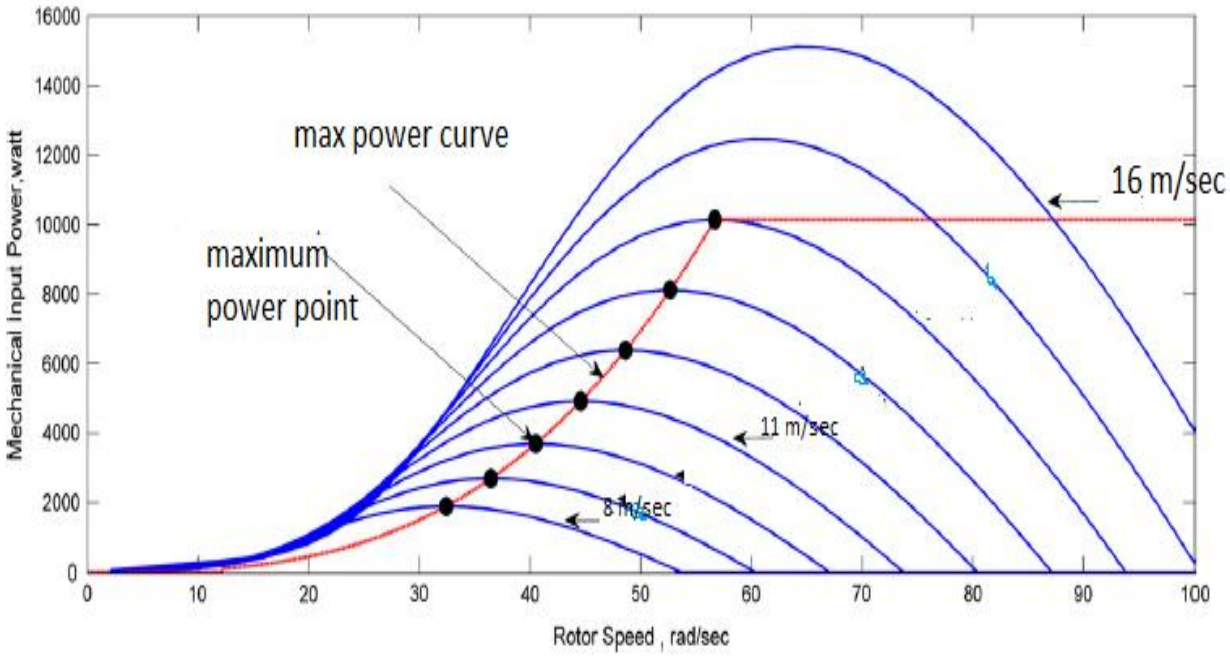


Fig.4.4 wind turbine power characteristics.

### 4.1.2 PMSG Modelling

PMSG transforms the mechanical power from the aerodynamic system into AC electrical power, which is subsequently transformed into dc power, using an IGBT based pulse width modulation (PWM) converter coupled to a dc connection at its dc port. The power is transmitted to the grid via another IGBT based pulse width modulation (PWM) inverter. The electrical model for the surface-mounted PMSG has been created. In the d-q rotating reference frame, it is frequently employed. Equivalent PMSG circuits in d-q axes are shown in Fig.4.5. The stator voltage ($V_{sd}$ , $V_{sq}$) are expressed in the d-q reference frame as;

$$V_{sd} = -R_s\ I_{sd} - L_s \frac{d}{dt} I_{sd} + L_s w_e I_{sq} \tag{4.5}$$

$$V_{sq} = -R_s\ I_{sq} - L_s \frac{d}{dt} I_{sq} - L_s w_e I_{sd} + \phi w_e \tag{4.6}$$

Where $w_e$ is the generator's electrical rotating speed , $L_s$ and $R_s$, stand for the PMSG stator winding inductance and resistance, $\phi$ for the magnetic flux, and $I_{sd}$ and $I_{sq}$ the machine currents' direct and quadrature components respectively .

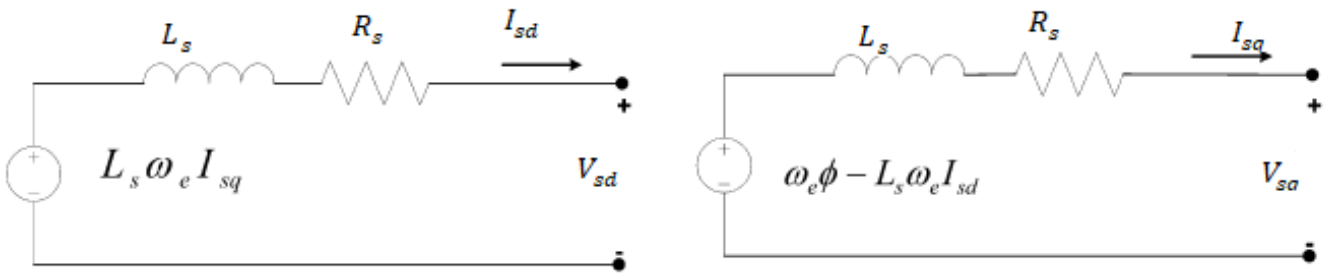


Fig.4.5 PMSG electrical circuit (i) d-axis (ii) q-axis.

The electromechanical torque ($T_e$),

$$T_e = \frac{3}{2} P I_{sq} \left( (L_d - L_q) I_{sd} + \phi \right) \tag{4.7}$$

P = Pole pairs,

In PMSG (surface mounted) $L_d = L_q = L_s$ , consequently, the electromagnetic torque ($T_e$) may be expressed once more as,

$$T_e = \frac{3}{2} P I_{sq} \phi \tag{4.8}$$

As we know that;

$$w_e = w_m P \tag{4.9}$$

$w_e$ = electrical rotational velocity

$w_m$ = mechanical rotational velocity of the rotor

### 4.1.3 Converters interfacing

According to Fig. 4.1, IGBT based back-to-back converters link PMSG to the electric grid. The first converter, also known as the generator side converter, is where the stator windings of said PMSG's are linked. The other, ac filter-connected grid side converter, is connected to the grid at the PCC. Shunt dc capacitor is used to collect the two converters' dc terminals. Each converter's power configuration consists just of a three-legged voltage source inverter (VSI). However

inverter switches can be controlled using a different types of control methods dependent on the control functions. Control methods for the two converters will be explained in the upcoming sections.

## 4.2 Machine side converter's control scheme

To get the maximum output power we will have to control the shaft speed of wind turbine. For this reason it is necessary to control machine side converter (MSC). Again the maximum output power depends on the power coefficient ( $C_p$ ) in a variable speed wind energy conversion system (WECS), at different wind speeds. However, $C_p$ is not constant for wind turbines. The tip speed ratio (λ) and pitch angle (β), as shown in Fig.4.3, are the variables that influence the coefficient$C_p$. The generator rotor speed must be maintained at $w_m$ to attain the ideal value of the tip speed ratio ($\lambda_{opt}$) in order for the wind turbine to produce the maximum amount of power ($P_{max}$) at $C_{p\_max}$ . According to the maximum power curve illustrated in Fig.4.4, if the wind speed changes, the rotor speed should be modified to match the change in the wind speed. Hence, the generator side converter is used to control the generator's speed ($w_m$). As a result, the generator can adjust its rotational speed in response to changes in incident wind through control of the machine-side converter (MSC).The discussion of the equation of motion is necessary to comprehend the control idea. The following is the motion equation for a common generator.

$$J\frac{dw_m}{dt} = T_m - T_e - Bw_m \tag{4.10}$$

Where, J is the system's total inertia (Kg $m^2$), which includes the turbine and generator, and B is the friction factor (N m s).

The PMSG rotor's mechanical rotational speed is determined by,

$$w_m = w_t G_r \tag{4.11}$$

Where, $w_t$ is the turbine's rotational speed and (if applicable) $G_r$ is the gear ratio.

$G_r = 1$ For gearless PMSG-based wind turbines.

According to equation (4.10), the electromagnetic torque regulates the generator's rotational speed, hence speed control is achieved by controlling the generator's torque. According to (4.8), the q-axis current component,$I_{sq}$, may directly affect the electromagnetic torque, and as a result, the speed may be adjusted by modifying the q-axis current component. To reduce current flow for a given electromagnetic torque and, consequently, resistive losses, the d-axis current component $I_{sd}$ is set to zero. As shown in Eqs. (4.5) and (4.6), the stator voltage, $V_{sd}$and$V_{sq}$, produced by the machine side converter (MSC), can be used to control the generator current components, $I_{sd}$ and, $I_{sq}$ in Eqs. (4.5) and (4.6). The controller needs feedback from the $I_{sd}$ and $I_{sq}$ components of the PMSG stator current. The PI controller's input is the difference between the measured and reference components' error.

Then, as illustrated in Fig.4.6, compensation factors indicated in Eqs. (4.5) and (4.6) are taken into account to guarantee stable and decoupled active and reactive power control. When switching signal needed to operate the machine side converter (MSC) is produced, by the output voltage that will be the input of space vector modulation (SVM).

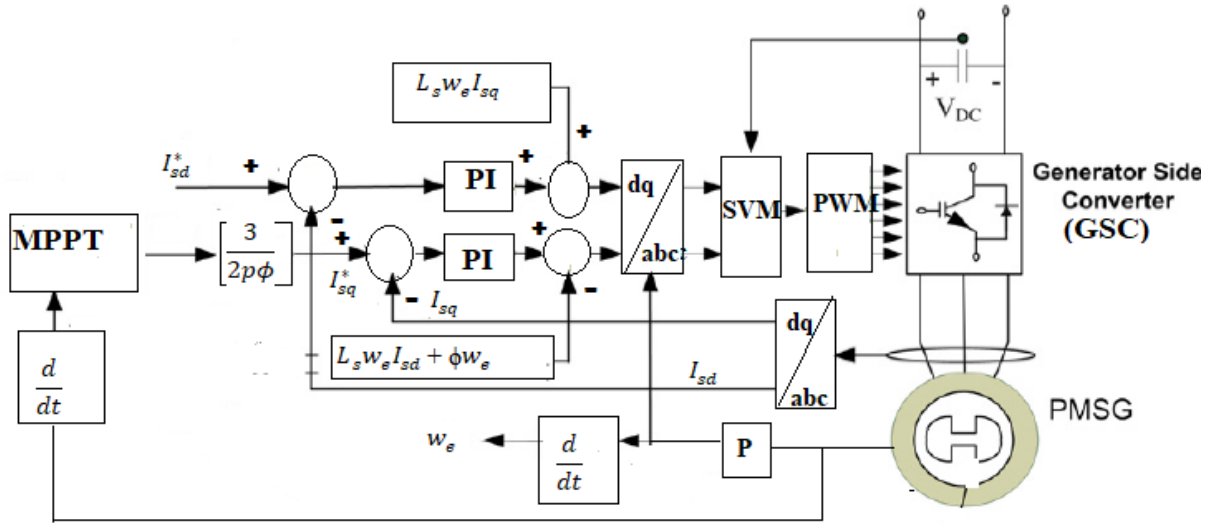


Fig .4.6 machine side converter block diagram.

## 4.3 Grid side converter

The grid side converter control's goal is to maintain the dc link voltage at its nominal level of 700V the value of the LL rms voltage ($V_{g-LL}$) observed on the grid side is related to the DC link voltage ($V_{DC}$). The relation is;

$$V_{DC} \geq 1.63V_{g-LL}$$

Consequently, during the operation of a wind turbine, making sure that the active power produced by the generator is fed into the grid where the capacitor voltage always fluctuates. It is important to note that different control mechanisms are employed to implement grid side converter depending on the reference frame. The synchronous reference frame control strategy is being looked into in this instance. Here is the dynamic model of the grid connection in a frame of reference that rotates synchronously with the grid voltage.

$$V_{gd} = V_{id} - RI_{gd} - L\frac{d}{dt}I_{gd} + Lw_gI_{gq} \quad (4.12)$$

$$V_{gq} = V_{iq} - RI_{gq} - L\frac{d}{dt}I_{gq} - Lw_gI_{gd} \quad (4.13)$$

Where, L and R stand for the corresponding inductance and resistance of the grid. The inverter voltage components are $V_{id}$ and$V_{ig}$. The grid vector voltage is if the reference frame is aligned along the supply voltage is

$$\text{V} = V_{gd} + j0 \quad (4.14)$$

Following are the equations of Active and Reactive power

$$P_g = \frac{3}{2}V_{gd}I_{gd} \quad (4.15)$$

$$Q_g = \frac{3}{2}V_{gq}I_{gq} \quad (4.16)$$

From the equations above, it is clear that by adjusting the d-axis and q-axis current components, respectively, we may change the active and reactive powers. Additionally, as stated in the following constraint, the dc-link voltage must remain constant in order to transfer all of the active power generated by the wind turbine.

$$C\frac{dV_{DC}}{dt} = \frac{P_t}{V_{DC}} - \frac{P_g}{V_{DC}} \quad (4.17)$$

Where, subscript g is grid and t is wind turbine

According to Eqn. (4.17), the dc-link voltage won't change if the two powers (the wind turbine power ($P_t$) and the grid power ($P_g$)) are equal.

Two cascaded loops are present in the grid side converter's control approach (shown in Fig.4.7). The outer loops regulate the dc-link voltage and reactive power, while the inner loops control the grid currents. The active and reactive power sent to the grid is managed by the outer loops, which also control the system's overall power flow. In addition, unless the grid operators require differing reactive power settings, unity power factor flow (zero reactive power exchange) might be easily attained.

The currents are represented in the dq synchronous rotating reference frame and controlled by conventional PI controllers in this control method. With this control, grid voltages and currents from the abc reference frame are converted to their equivalents in the dq reference frame. It's important to note that the transformation of the ABC variables into DC components (or DQ components) makes controllability simpler and more practical. Since they perform well for regulating dc variables, the control structures created in this study use PI controllers. The second channel regulates reactive power by generating an ($I_{gq}$) reference to the inner current control loop. The reactive power has been set to zero.

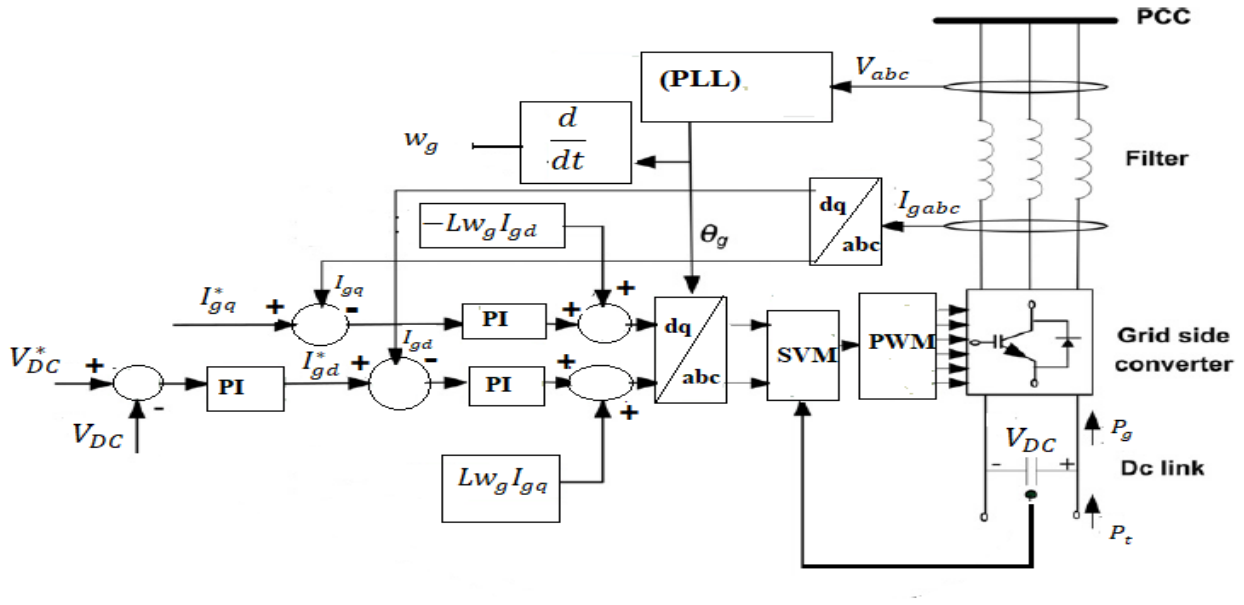


Fig 4.7 Grid side converter block diagram

# Chapter 5

# Results and Discussion

The MATLAB/Simulink has been used to simulate the proposed scheme of Hybrid system topology.

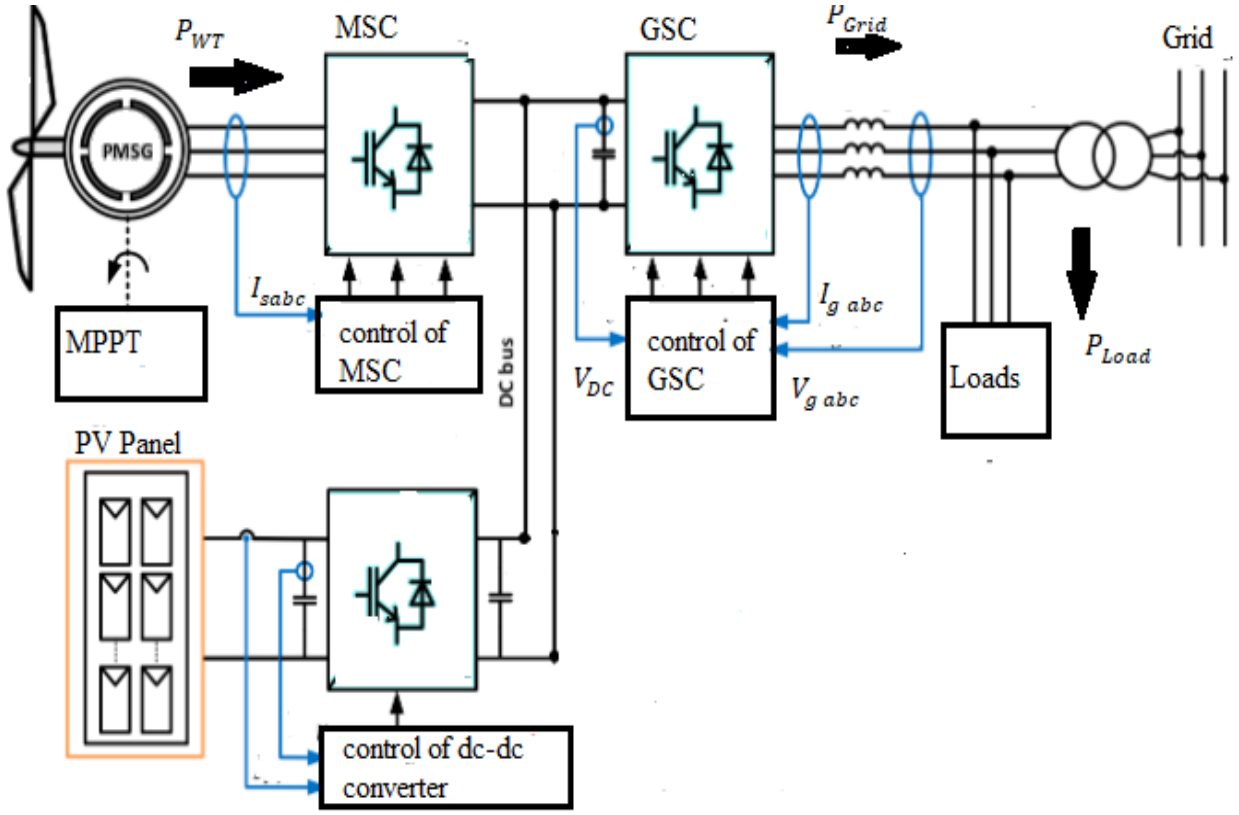


Fig 5.1 Block diagram of model

Fig. 5.1 shows the block diagram of proposed technique used for integration of PMSG based WECS with PV array connected to the grid using back to back converter.

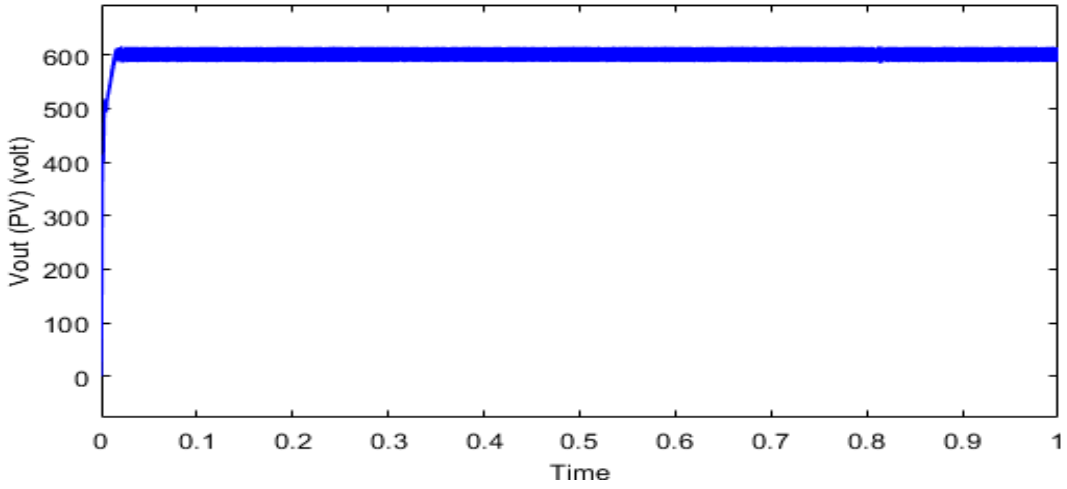


Fig .5.2 output voltage of PV array

Fig. 5.2 shows the output voltage of PV array when the solar irradiance is ($900^{W}/_{m^2}$)

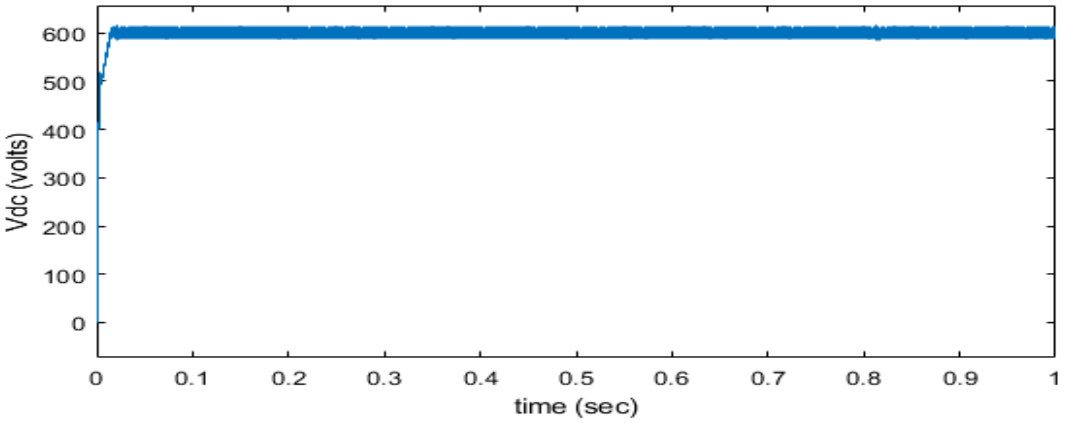


Fig 5.3 Vdc vs. time.

Fig 5.3 shows the voltage at DC link when wind speed is 13m/sec.

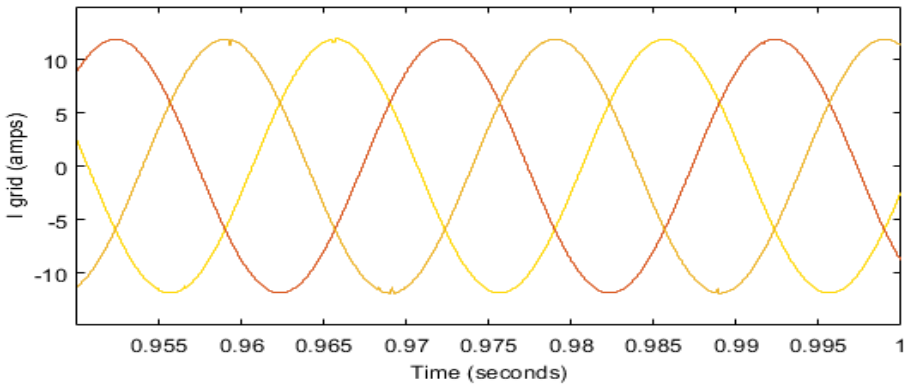


Fig 5.4 Grid current vs. time.

Fig 5.4 shows the grid current when the speed of wind is 13m/s and solar irradiance is ($900^{W}/_{m^2}$)

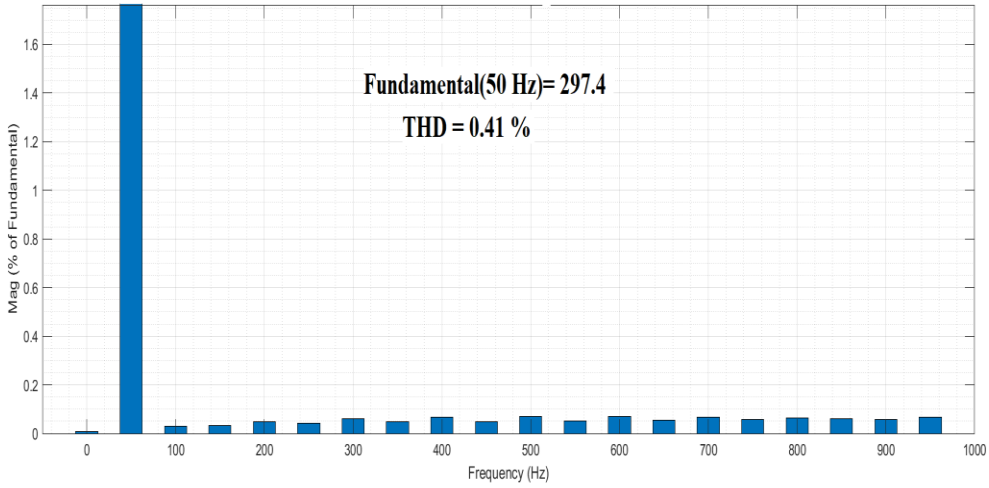


Fig 5.5 THD of grid current phase 'a'.

Fig 5.5 shows the %THD of phase 'a' of the grid current when the speed of wind is 13m/s and solar irradiance is ($900^{W}/_{m^2}$)

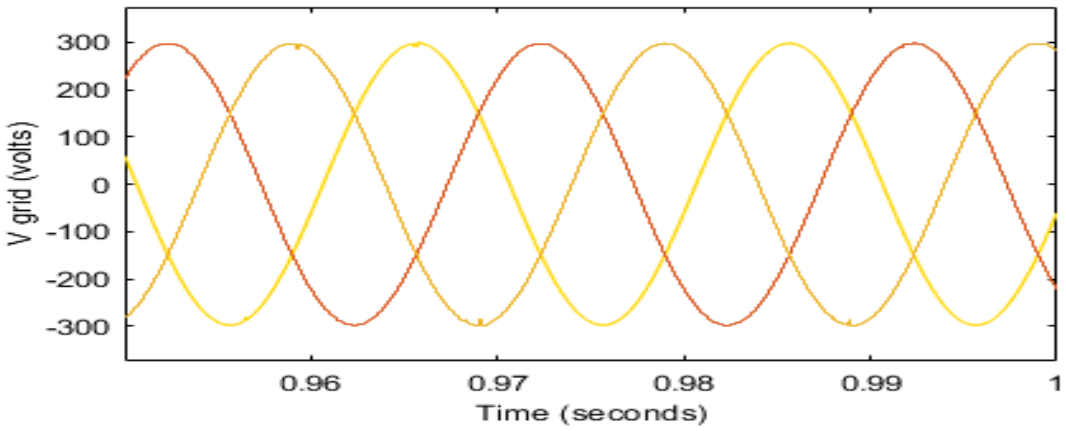


Fig 5.6 Grid voltage vs. time.

Fig 5.6 shows the grid voltage when the speed of wind is 13m/s and solar irradiance is ($900^{W}/_{m^2}$)

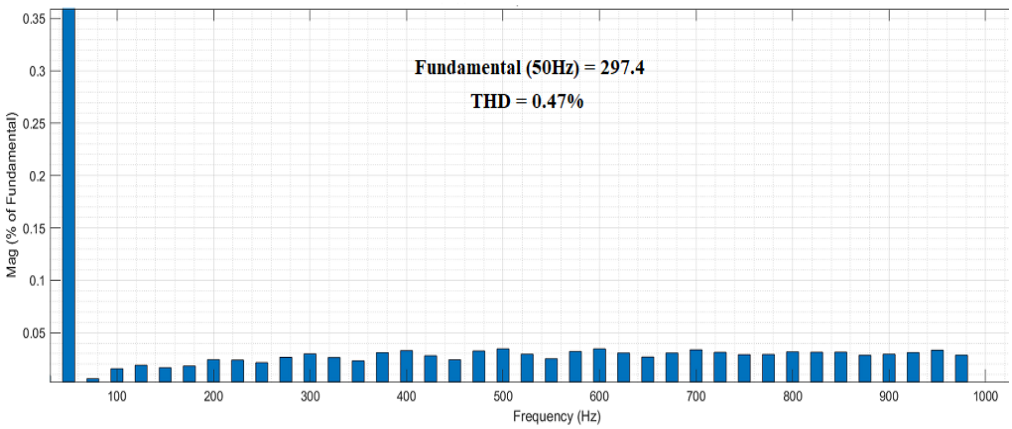


Fig 5.7 THD of grid voltage of phase ‘a’.

Fig 5.7 shows %THD of phase ‘a’ of the grid voltage when the speed of wind is 13m/s and solar irradiance is ($900^{W}/_{m^2}$)

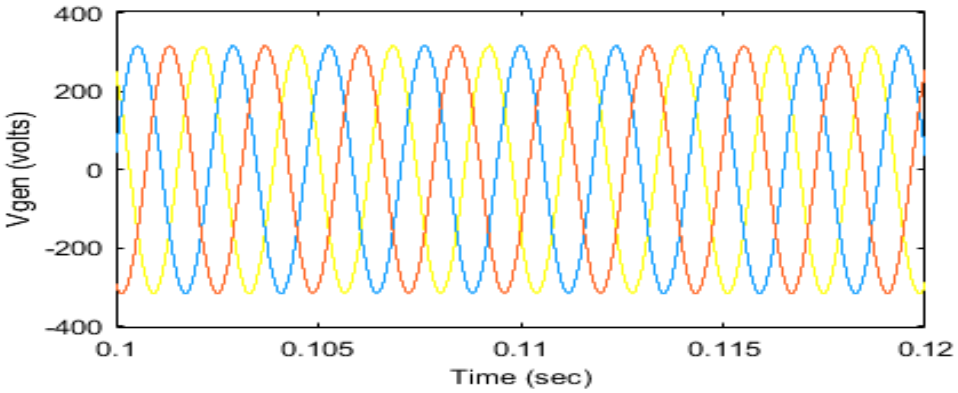


Fig 5.8 Generator voltage vs. time.

Fig 5.8 shows the generator voltage when the speed of wind is 13m/s and solar irradiance is $(900^{W}/_{m^2})$

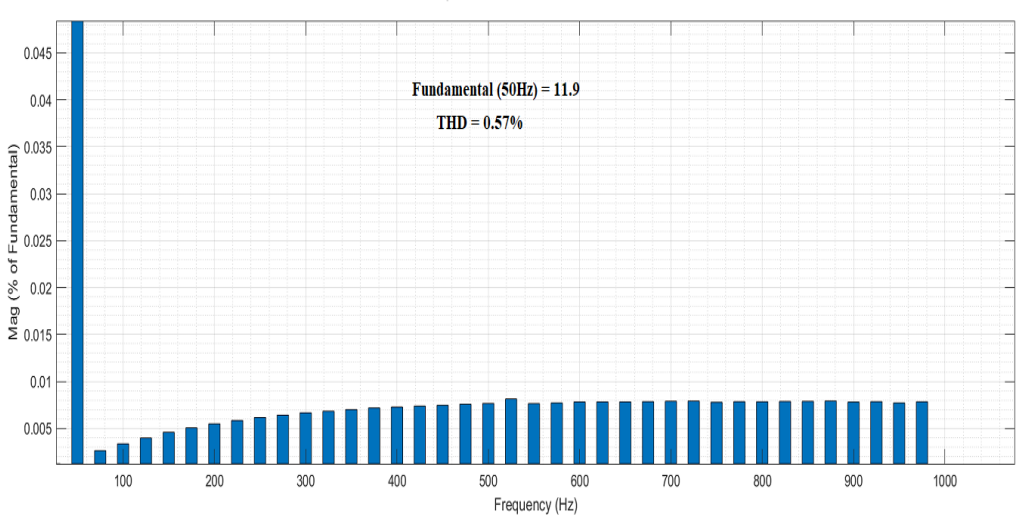


Fig 5.9 THD of generator voltage of phase ‘a’.

Fig 5.9 shows the %THD of phase ’a’ of the generator voltage when the speed of wind is 13m/s and solar irradiance is $(900^{W}/_{m^2})$

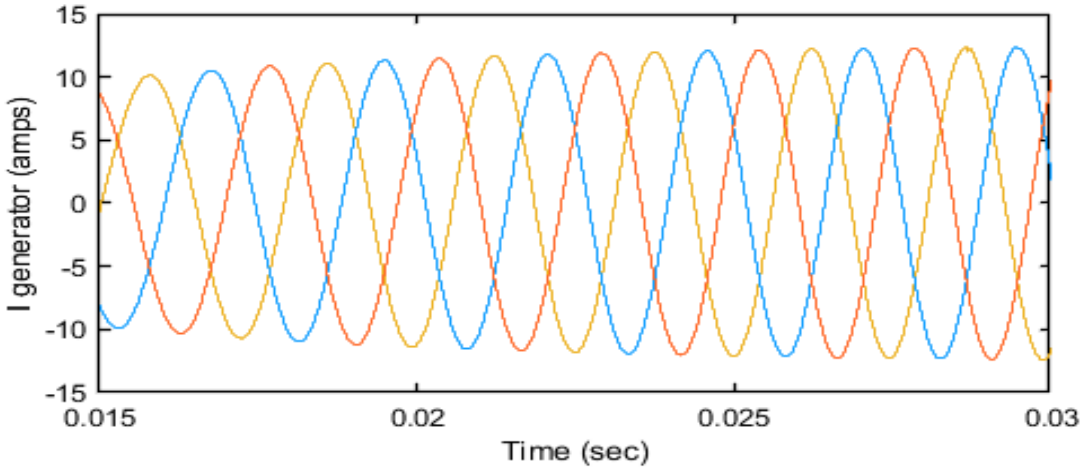


Fig 5.10 Generator current vs. time.

Fig 5.10 shows the generator current when the speed of wind is 13m/s and solar irradiance is ($900^{W}/_{m^2}$)

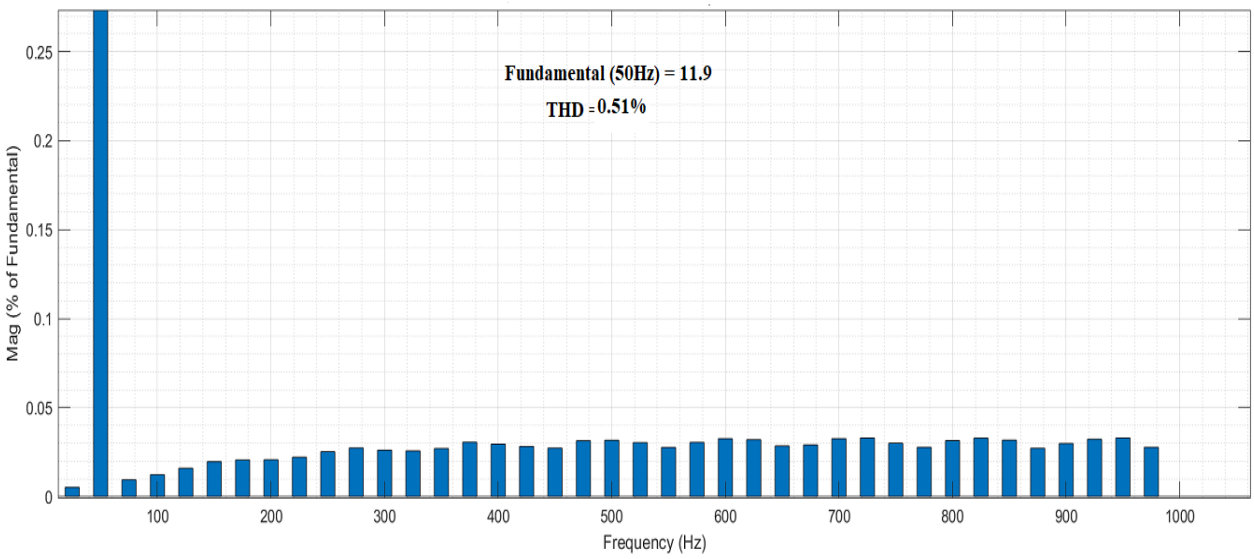


Fig 5.11 THD of generator current of phase ‘a’.

Fig 5.11 shows the %THD of phase ‘a’ of generator current when the speed of wind is 13m/s and solar irradiance is ($900^{W}/_{m^2}$)

Table 5.1. %THD of voltage

| | Generator voltage (%) | Grid voltage (%) |
|---|---|---|
| Phase ‘a’ | 0.57 | 0.47 |
| Phase ‘b’ | 0.62 | 0.38 |
| Phase ‘c’ | 0.62 | 0.41 |

Table 5.2. %THD of current

| | Generator current (%) | Grid current (%) |
|---|---|---|
| Phase ‘a’ | 0.51 | 0.41 |
| Phase ‘b’ | 0.68 | 0.41 |
| Phase ‘c’ | 0.63 | 0.39 |

## Discussion

As we know that the speed of the wind and intensity of the sun changes continuously, at normal condition during the day time intensity of the sun will be higher and at night speed of the wind will be more. so to maintain the grid voltage and frequency at nominal value we are using the master and slave technique when the dc link voltage at shunt capacitor of back to back converter is higher than output voltage of PV array , that time PMSG based WECS will supply the power to grid , vice- versa . In this proposed model we are considering the speed of the wind is increasing and intensity of the sun light is decreasing continuously. At a point when the speed of wind is 13m/s and the solar irradiance is ($900 {}^{W}/_{m^2}$) , both the dc link voltage and the output voltage of PV array are same around 620V. At this point voltage and current of the grid and the generator,$V_{DC}$ and output voltage of PV array are shown in the result. The THD of grid voltage and generator voltage are less than 5% as per IEEE standard of maintaining power quality. The THD of grid current and generator current are also below 5%and maintaining IEEE standards of power quality. The THD of current and voltage of grid and generator side is shown in table.5.1 and table 5.2.

# Chapter 6

# Conclusion and Future scope

## Conclusion

In this proposed model back to back converter has been used in PMSG based wind energy conversion system and dc boost converter in PV array model. In PMSG based wind energy conversion system machine side converter (MSC) control is mainly implemented to maximize output power by controlling the speed of the turbine shaft and the grid side converter (GSC) control is used to maintain the dc link voltage by using the relation ($V_{DC} \geq 1.633 V_{g-LL}$) and ensuring the active power generated by the generator is supplied to the utility grid .The maximum power point of operation is tracked for both the system using P&O algorithm. The total harmonic distortion is also maintained below 5% as per IEEE standards.

## Future scope

1. Different algorithm can also be used to track MPP.
2. From the point of view of protection, the control system should consider the circumstance of over load or over current in the future.
3. For the grid side inverter, the next step should consider how to inject the reactive power current into the grid for the purpose of stabilising the power grid.
4. This proposed scheme can be improved further using different converters.
5. Battery storage system can be also used, when there will be surplus power supply battery will charge and battery will discharge in case of power deficit to maintain the stability of power grid.

# APPENDIX

**A.** The coefficient $C_1$ to $C_6$

| | |
|---|---|
| $C_1$ | 0.5176 |
| $C_2$ | 116 |
| $C_3$ | 0.4 |
| $C_4$ | 5 |
| $C_5$ | 21 |
| $C_6$ | 0.0068 |

**B.** Specification of the wind turbine

| | |
|---|---|
| Blade length of wind turbine ( r ) | 2 m |
| Air density (ρ) | 1.225 $kgm^3$ |
| tip speed ratio optimum ($\lambda_{opt}$) | 8.2 |
| Maximum power coefficient ($C_{p\,max}$) | 0.48 |

**C**. Parameters of the generator (PMSG)

| | |
|---|---|
| Stator resistance ($R_S$) | 0.0083Ω |
| Direct axis inductance ($L_{Sd}$) | 0.172mH |
| Quadrature axis inductance ($L_{Sq}$) | 0.172mH |
| Permanent magnet flux (ϕ) | 0.089wb |
| Inertia of system (J) | 0.071$Kgm^2$ |
| Friction factors (B) | 0.005Nm |
| Pole pairs (P) | 6 |

**D.** Grid and DC bus parameters

| | |
|---|---|
| DC link capacitance (C) | 8000μF |
| Grid frequency (f) | 50Hz |
| Grid resistance ($R_g$) | 0.025 Ω |
| Grid inductance ($L_g$) | 0.05mH |

**E.** PI parameters

| | |
|---|---|
| Machine side converter current loop | $K_P$ = 0.1<br>$K_I$ = 100 |
| Grid side converter current loop | $K_P$ = 2.5<br>$K_I$ = 500 |
| DC link loop | $K_P$ = 0.002<br>$K_I$ = 0.05 |

# REFERENCES


[1] T. Salmi, M. Bouzguenda, A. Gagtli, "MATLAB/Simulink based modeling of solar photovoltaic cell," *International journal of renewable energy research,* vol.2, no.2, 2012.

[2] S. Meenakshi, K.Rajambal, S. Elangovan "Intelligent controller for stand-alone hybrid generationsystem," *IEEE,* May. 2006.

[3] Nabil A. Ahmed, Masafumi Miyatake, "A stand-alone hybrid generation system combining solar photovoltaic and wind turbine with simple maximum power point tracking control," *IPEMC* 2006, *IEEE,* 2006.

[4] M. G. Villalva, J. R. Gazoli, "Modeling and circuit based simulation of photovoltaic arrays," *Brazilian power electronics conference (COBEP),* 2009.

[5] Marcelo Gradella Villalva, Jonas Rafel Gazoli, "Comprehensive approach to modeling and simulation of photovoltaic arrays," *IEEE transaction on power electronics,* vol.24, no.5, May 2009.

[6] Tan K, Islam S. Optimum control strategies in energy conversion of PMSG wind turbine system without mechanical sensors. IEEE Trans Energy Convers 2004.

[7] Baroudi JA, Dinavahi V, Knight AM. A review of power converter topologies for wind generators. Renew Energy 2007; 32(January):2369–85.

[8] SiyuGuo, Timothly Michael Walsh, "Analyzing partial shading of PV module by circuit modeling," *IEEE* 2011.

[9] Zhou Xuesong, Song Daichun, Ma Youjie, Chen Deshu, "The simulation and design for MPPT of PV system based on Incremental conductance method," *Wase International conference on information engineering,* 2010.

[10] Azadeh Safari, Saad Mekhilef, "Simulation and Hardware Implementation of Incremental Conductance MPPT with Direct Control Method Using Cuk Converter," *IEEE transaction on industrial electronics,* vol. 58, no. 4, April 2011

[11] Mihnea Rosu-Hamzescu, Sergiu Oprea, "Practical guide to implementing Solar panel MPPT algorithm," *Microchip technology Inc.,* 2013.

[12] M. Gengaraj, J. Jasper Gnanachandran, "Modeling of a standalone photovoltaic system with charge controller for battery energy storage system," *International Journal of Electrical Engineering,* vol.6, no. 3, 2013.

[13] T. Taftichat, K. Agbossou, "Output power maximization of a permanent magnet synchronous generator based stand-alone wind turbine system," *IEEE ISIE* July 9-6 2006.

[14] Roger Gules, Juliano De pellegrin Pacheco, "Maximum power point tracking system with Parallel connection for PV stand-alone application," *IEEE transaction on industrial electronics,* vol.55, no.7, July 2008.

[15] S. Rahmani, Ab. Hamadi, A. Ndtoungou, "Performance evaluation of a PMSG-based variable speed wind generation system using maximum power point tracking," *IEEE electrical power and energy conference* 2012.

[16] Majid Jamil, Ravi Gupta, "A review of power converter topology used with PMSG based wind power generation," *IEEE,* 2012.

[17] Eftichios Koutroulis, Kostas Kalaitzakis, "Design of a maximum power tracking system for wind-energy conversion application," *IEEE Transaction on industrial electronics,* vol. 53, no.2, April 2006.

[18] Chinchilia M, Arnaltes S, Burgos J. Control of permanent-magnet generator applied to variable-speed wind-energy systems connected to the grid. IEEE Trans Energy Convers 2006.

[19] Hu W, Chen Z, Wang Y, Wang Z. Flicker mitigation by active power control of variable-speed wind turbines with full-scale back-to-back power converters. IEEE Trans Energy Convers 2009.

[20] Iov F, Hansen AD, Sorensen P, Blaabjerg F. Wind turbine blackest in Matlab/Simulink, Research Project, Institute of Energy Technology, Alborg University, March 2004.